

~~CONFIDENTIAL~~

NACA RM L53J28



# RESEARCH MEMORANDUM

AN EXPERIMENTAL INVESTIGATION OF THE  
TRANSONIC-FLOW-GENERATION AND SHOCK-WAVE-REFLECTION  
CHARACTERISTICS OF A TWO-DIMENSIONAL WIND TUNNEL WITH  
24-PERCENT-OPEN, DEEP,  
MULTISLOTTED WALLS

By Thomas B. Sellers, Don D. Davis, and George M. Stokes

CLASSIFICATION CHANGED  
UNCLASSIFIED Langley Aeronautical Laboratory  
Langley Field, Va.

**LIBRARY COPY**

DEC 16 1953

LANGLEY AERONAUTICAL LABORATORY  
LIBRARY, NACA  
LANGLEY FIELD, VIRGINIA

by authority of NACA Res also  
+ RW-118 Date effective  
July 26, 1957  
AMT 9-12-57  
CLASSIFIED DOCUMENT

This material contains information affecting the National Defense of the United States within the meaning of the espionage laws, Title 18, U.S.C., Secs. 793 and 794, the transmission or revelation of which in any manner to an unauthorized person is prohibited by law.

## NATIONAL ADVISORY COMMITTEE FOR AERONAUTICS

WASHINGTON  
December 10, 1953

~~CONFIDENTIAL~~

## NATIONAL ADVISORY COMMITTEE FOR AERONAUTICS

## RESEARCH MEMORANDUM

3 1176 01357 2301

AN EXPERIMENTAL INVESTIGATION OF THE  
TRANSONIC-FLOW-GENERATION AND SHOCK-WAVE-REFLECTION  
CHARACTERISTICS OF A TWO-DIMENSIONAL WIND TUNNEL WITH  
24-PERCENT-OPEN, DEEP,  
MULTISLOTTED WALLS

By Thomas B. Sellers, Don D. Davis, and George M. Stokes

## SUMMARY

The flow-generation and shock-wave-reflection characteristics of a two-dimensional tunnel with 24-percent-open, deep, multisloTTed walls have been studied. The flow-generation tests included Mach numbers from 0.80 to 1.32 and slotted-wall divergence angles of 0', 20', and 40'. The shock-wave-reflection characteristics were studied for two shock strengths which resulted in Mach number decrements of 0.07 and 0.12 at a free-stream Mach number of 1.278. Suction outflows which were required to generate the test-section flow were measured for the Mach number and divergence-angle range.

Under the test conditions, the deep multisloTTed wall proved unsatisfactory as a means of reducing boundary-reflected disturbances, because a mixed disturbance was reflected from the wall. This disturbance consisted of a weak compression wave followed by a strong expansion wave and then a strong compression region.

The flow-generation tests showed that slight wall divergence improved the center-line velocity distribution near a Mach number of 1.3. Also, diverging the tunnel walls reduced the suction power required to generate a given Mach number. At subsonic speeds, the velocity distribution near the diffuser entrance is a function of the mass of air removed by suction.

## INTRODUCTION

In the low supersonic Mach number range, the presence of boundary-reflected disturbances in transonic wind tunnels has resulted in the

reduction of model size and a lack of interference-free data near a Mach number of 1. Each transonic tunnel is limited to a supersonic interference-free test-section length which is governed by the particular Mach number testing range and the axial distance required for the bow shock wave from the model to travel to the wall and reflect back to the tunnel center line. The magnitude and locations of these boundary-reflected disturbances in a typical slotted transonic wind tunnel are reported in reference 1.

The preliminary investigations reported in references 2 and 3 indicated that a reduction in the strength of wall-reflected disturbances could be obtained by employing a porous-wall wind tunnel with the correct uniform porosity. In order to investigate more extensively the general shock-wave reflection phenomena, a study was undertaken in a 3- by 3-inch transonic flow apparatus. For this program a two-dimensional test section was constructed with 24-percent-open, deep, multislotted, top and bottom walls. The multislotted type of wall was selected as an initial exploratory effort which more nearly approached a homogeneous porous wall than the existing slotted walls of the slotted NACA transonic tunnels. The 24-percent-open ratio was chosen on the basis of a preliminary determination of the normal-flow-porosity characteristics of similar test samples and the theoretical outflow requirements for shock-wave cancellation (refs. 2 and 3) at a Mach number of 1.28. The slotted walls were also used to generate the supersonic flow, instead of solid nozzle blocks, in order to eliminate the problems associated with a juncture of two dissimilar tunnel walls just ahead of the test region.

The wave-reflection characteristics for this slotted-wall configuration were investigated at a Mach number of 1.28 with two different shock-wave strengths. The transonic-flow-generation characteristics of these walls and the effect of wall divergence on the center-line velocity distribution were investigated for a Mach number range of 0.8 to 1.3 and slotted-wall divergence angles of 0', 20', and 40'. Air was removed through the slotted wall by means of a separate source of suction and tests were made to determine the mass flow removed in order to generate various Mach numbers over the wall-divergence-angle range.

#### SYMBOLS

H	total pressure in tunnel upstream of test section, lb/sq ft
M	Mach number
$\Delta M$	decrement in Mach number across incident shock wave
m	total mass flow in wind tunnel

$\Delta m$	suction mass flow
P	static pressure, lb/sq ft
x	axial distance, in.
z	vertical distance, in.

## EQUIPMENT AND APPARATUS

### Basic Tunnel Circuit

The photographs in figure 1 and the schematic diagram of figure 2 show the transonic flow apparatus which is a two-dimensional transonic wind tunnel with a 3-inch by 3-inch throat. The basic tunnel is a single-return, closed-circuit, continuously operating type of wind tunnel which is powered by a single-stage, variable-speed, aircraft-engine type of supercharger. The maximum pressure ratio produced by this main-drive supercharger is 2.2 at a flow quantity of 80 cubic feet of standard air per second. The supercharger is driven by a 250-horsepower, air-cooled, squirrel-cage induction motor with speed controlled by means of a variable-frequency power supply.

The tunnel circuit was covered with a 3-inch thickness of asbestos which reduced the amount of heat radiation from the steel shell. The tunnel stagnation air temperature was maintained at 200° F by an air exchanger shown in the photograph of figure 1(a) and in the schematic of figure 2. The intake air was drawn in through an air filter from the atmosphere.

### Suction Equipment

In this tunnel, air was removed from the test section plenum chamber by a separate source of suction. With this arrangement, the suction control was entirely independent of the main tunnel drive, and furthermore, the mass of air removed from the test section was easily measured. The arrangement of the suction equipment is shown in figure 2. The source of suction was a two-stage, two-speed, aircraft-engine-type supercharger which was driven by two 200-horsepower, water-cooled induction motors. The suction equipment was capable of a maximum pressure ratio of 5.6 at a flow quantity of 40 cubic feet of standard air per second. The speed was controlled by means of a variable-frequency power supply similar to that which was used for the main-drive supercharger.

The air removed from the test section was carried through separate 3-inch-diameter pipes which were connected to the top and bottom plenum

tanks (fig. 1(b)) and through a transition duct into a 6-inch-diameter circular duct to the inlet of the suction supercharger. A calibrated orifice plate which was used to determine the suction mass flow was located in the 6-inch duct. Manually operated gate valves, which permitted separate regulation of the pressure in each plenum tank, were located in the 3-inch-diameter pipes. In order to determine the tank pressure, flush static-pressure orifices were located in the walls of each tank.

Because the small mass of air removed from the test section was insufficient to prevent the suction supercharger from surging, a separate bleed into the supercharger inlet was required. The air bled into the system was taken from the atmosphere and the quantity of air was controlled by a manually operated 3-inch gate valve which was located in the bleed ducting. This valve was set for nonsurging operation at a maximum pressure ratio condition and was locked at this setting.

#### Test Section

The removable test section extends from the entrance cone (station -3 in fig. 3(a)) to the diffuser (station  $13\frac{1}{8}$ ) and is constructed in a manner which permits various porous nozzle configurations to be installed without altering the basic-test-section structure. Figure 3 presents the overall dimensions and general details of this construction. The test-section top and bottom walls were 24-percent-open, deep, slotted walls which were made up of 73,  $1/32$ -inch-thick 1-inch-wide steel plates stacked as shown in figure 3(a). The plates were located with 0.010-inch slots between plates, but, in order to span the 3.019-inch-wide tunnel, the two slots at the side walls were made 0.015-inch wide. The stacked plates extended from station  $-\frac{5}{16}$  to station  $13\frac{1}{8}$ . The entire stacked-plate wall was supported by  $1/4$ -inch-thick steel side rails and the plates were held together with three rows of  $1/16$ -inch-diameter rods which were located  $5/8$  inch below the tunnel wall surface and passed through the stacked plates into the side rails. The rods were threaded on each end and secured in place with nuts. The spacing between plates was obtained with 0.010-inch-thick  $1/8$ -inch-diameter spacers which were fitted over each rod between each plate.

In the region from station  $-5/16$  to 1, flow guides were inserted between the stacked plates with the result that the distance between the tunnel wall surface and the flow guide gradually increased. The contours of the two flow guides tested are presented in figure 3(b). It should be noted from these contours that the slots begin to open at station 0, not  $-5/16$ . The juncture at the intersection of the stacked-plate wall and flexure plate was made fair and smooth.

The test-section construction allowed the top and bottom walls to be independently diverged from the parallel condition to an angle of 60' of divergence for each wall. The diverging of the walls was accomplished by means of the wall-positioning jack screws which were attached to the flexure plates. Bending the flexure plates caused the slotted wall to diverge because the steel side rails of the stacked plate walls were securely fastened to the flexure plates. Once the walls were positioned on the correct angle, the walls were locked in place by the wall-locking screws. A pivoted pointer was attached by mechanical linkage to each wall and the divergence-angle settings were calibrated by the movement of this pointer. Figure 1(c) shows this pointer arrangement and the wall-diverging mechanism. The glass side walls, which permitted schlieren observation, were bonded into steel window frames and were mounted on the removable test section with the glass walls parallel. The window units were removable to permit probe changes and model installation.

#### Model

The model was a two-dimensional plain wedge 3 inches in length with a 5° apex angle (fig. 3(a)). Nine flush static-pressure orifices were located every 0.3 inch on the bottom surface of the wedge. Support shafts 0.205 inch in diameter were located  $1\frac{1}{2}$  inches from the wedge apex and extended from each side of the wedge. In order to mount the model in the glass side walls, a 5/16-inch-diameter hole was drilled through the glass wall and a plastic bushing was inserted into the hole in the glass. This plastic bushing was drilled to fit the model shafts. In order to install the model in the tunnel, one side wall was removed, the model shafts were inserted in the plastic bushings, and the glass wall was replaced.

#### Probes

Figure 4 presents the details of the 0.040-inch-diameter movable static probe. The 0.040-inch-diameter static-pressure tube was supported by a 1/4-inch-diameter rod. The pressure tube extended beyond the rear of the rod into the diffuser and out the tunnel wall to a manometer. The movable static probe could be moved longitudinally and vertically from outside the diffuser.

The center-line probe, as shown in figure 4, was mounted along the tunnel center line by means of streamlined strut supports located in the tunnel entrance cone and diffuser. The center-line probe consisted of a 1/4-inch-diameter stainless-steel tube that contained nine 0.010-inch-diameter flush static orifices. The orifices were located 2 inches apart

and, in order to allow the complete static-pressure survey, the probe could be moved 2 inches along the tunnel center line. This movement allowed complete static-pressure surveys from station -4 to station 14.

### Schlieren Apparatus

The schlieren apparatus consisted of a point source of light, two 8-foot-focal-length parabolic mirrors, 12 inches in diameter, a movable crosshead and knife-edge arrangement, and a ground-glass viewing screen. A schematic diagram of this system is presented in figure 5.

A water-cooled mercury-vapor light source was used. After passing through a focusing lens, the light beam was directed through a 0.010-inch-diameter orifice and upon mirror A and then through the test section to mirror B. From mirror B, the light was focused on the knife edge and then was reflected from a plain mirror to the ground-glass screen. Schlieren photographs were taken with 1/5-second exposure time.

## TESTS AND PROCEDURES

### Flow-Generation Tests

In the center-line velocity-distribution tests, the tunnel-wall divergence angle was held constant and the Mach number was varied through the Mach number range. The center-line Mach numbers were determined by the static-pressure measurements which were obtained with the center-line probe (fig. 4) at 1/4-inch axial intervals from station -4 to 14. Center-line Mach number distributions were determined with flow guides 1 and 2 installed in the slotted wall. The contours of these flow guides are presented in figure 3(b). The term "basic wall configuration" will refer to the test section with flow guide 1 installed. Center-line Mach number distributions were also determined with a wall restriction which was a screen woven of eighty 0.004-inch-diameter wires per inch one way and seven hundred 0.003-inch-diameter wires per inch the other way. The restriction spanned the back surface of the slotted wall and extended from station 1.125 to 4.125. The mass of air removed through the slotted walls was determined for the range of Mach numbers and divergence angles tested. For these tests the pressure differential over a calibrated orifice plate was used to determine the mass flow removed for each condition.

### Wave-Reflection Tests

For the wave-reflection tests, a two-dimensional,  $5^{\circ}$ , 3-inch-chord wedge model was mounted on the tunnel center line with the model leading

edge located at station  $8\frac{1}{8}$ . The model solid blockage was 8.9 percent of the tunnel area with the walls diverged 20'. Reflection tests were made at a free-stream Mach number of 1.278 and at 20' of wall divergence with the model set at angles of attack of approximately  $1/2^\circ$  and  $1^\circ$ .

In studying the wave-reflection characteristics of the 24-percent-open, deep, slotted wall, three longitudinal-static-pressure surveys were taken at vertical locations of  $1/2$ ,  $3/4$ , and 1 inch from the tunnel center line. These surveys included the flow region from upstream of the model leading-edge shock to a point downstream of the reflected wave. The static-pressure measurements were taken with the movable static probe (fig. 4). In conjunction with the flow surveys, the wedge surface pressures were determined at nine stations.

### Schlieren Pictures

Qualitative data were obtained with the schlieren apparatus described in the equipment and apparatus section. Schlieren photographs which show vertical and horizontal density gradients were taken during the tests. Care was taken in selecting high-quality optical glass for the tunnel glass side walls and in adjusting the sensitivity of the schlieren system in order to obtain the greatest amount of the flow detail.

## RESULTS AND DISCUSSION

### Flow Generation

In this paper the flow-generation characteristics of the multislot wall will be presented first in order to establish the uniformity of the flow in the region of the test section where the wave-reflection tests were conducted. The center-line Mach number distributions with the multislot walls set at divergence angles of 0', 20', and 40' over a range of Mach numbers from  $M = 0.8$  to 1.3 are presented in figure 6.

Tunnel walls parallel.- Generally, for the parallel-wall case (fig. 6(a)), three flow-development ranges which were identified by the average Mach number from  $x = 8$  inches to  $x = 11$  inches were evident as the Mach number was increased. These ranges were  $M = 0.816$  to 1.030,  $M$  near 1.128, and  $M = 1.219$  to 1.320. In the low Mach number range from  $M = 0.816$  to 1.030, the flow was rapidly accelerated and the final Mach number was established within an axial distance of 1 tunnel height ( $x = 3$  inches) from the origin of the slots. In the moderate Mach number range,  $M$  near 1.128, the initial flow expansion created a maximum Mach number near the value of the final Mach number, but an undesirable

expansion-compression wave was created at the upstream end of the slots. This expansion-compression wave resulted in a cyclic center-line velocity distribution. Although the magnitude of the cyclic variation was reduced as the flow progressed downstream, variations were present throughout the length of the test section. In the high Mach number range from  $M = 1.219$  to  $1.320$ , the initial flow acceleration reached a maximum Mach number which was less than the final Mach number and again the expansion-compression wave was present, but, in contrast with the flow in the moderate Mach number range, the cyclic-flow variations were more quickly damped. The cyclic-flow variations were not present in the rear portion of the test section at  $M = 1.32$  but a general flow acceleration was present in this region. The presence of this flow acceleration indicated that the slotted walls were too dense to produce an equilibrium center-line velocity condition in the available length.

In summation, although the maximum Mach number variation in the flow generated by the multislot test section was within  $\pm 0.005$  up to  $M = 1.219$  in the region from  $x = 8$  inches to  $x = 11$  inches, the flow expansion-compression wave at Mach numbers greater than  $1.03$  and the flow acceleration in the rear of the test section ( $x = 8$  inches to  $x = 11$  inches) at  $M = 1.32$  were undesirable.

Effect of divergence.- As a possible means of eliminating the flow acceleration located from  $x = 8$  inches to  $11$  inches at the high Mach numbers, the tunnel walls were diverged from  $0'$  to  $20'$  and  $40'$ . Diverging the top and bottom tunnel walls resulted in a forward movement of the sonic point (figs. 6(b) and 6(c)). A study of the wall-divergence mechanism (fig. 3(a)) indicates that this shift in the location of the sonic point was due to the physical bending characteristic of the tunnel flexure plate. As the walls were diverged, the station for minimum distance between the flexure plates moved upstream; this resulted in a similar movement of the sonic point. Therefore, the flow was supersonic upstream of the intersection of the flexure plate and the slotted-wall assembly (station -  $\frac{5}{16}$ , fig. 3(a)). Although the juncture appeared smooth, undoubtedly a discontinuity did exist because the shock wave which was seen near  $x = 0$  as a sharp decrease in velocity in the diverged cases was traced to station -  $\frac{5}{16}$ .

Increasing the tunnel-wall divergence angle did not alter the rate of the initial flow expansion due to the slots, but the magnitude of the initial expansion increased with increasing wall divergence angle. Also the flow acceleration at  $x = 8$  inches to  $11$  inches which was present near  $M = 1.3$  with the walls parallel was reduced as the walls were diverged. Although increasing the divergence angle altered the magnitude of the various flow characteristics, the general flow pattern was qualitatively similar for the divergence angles tested.

It is of interest to note that the three general flow-development ranges discussed in the previous section were also evident with the walls diverged. A study of the data at the supersonic Mach numbers at the three divergence angles indicates that the strength of the cyclic-flow variations was determined by the magnitude of the initial expansion-compression wave, the Mach number, and the porosity characteristics of the slotted wall. Specifically, the magnitude of the expansion-compression wave determined the initial amplitude of the oscillations; the Mach number determined the axial distance required to complete 1 cycle of the oscillation; and the wall porosity characteristics determined the number of cycles necessary to damp the disturbance. In the Mach number region near 1.12, these three factors combined to create an oscillation which extended throughout the test section at all divergence angles tested.

This oscillation is apparent not only in the velocity-distribution plots, but also in schlieren photographs. Figure 7(a) is a schlieren photograph of the flow at  $M = 1.12$  with  $20^\circ$  of wall divergence. The oscillation is clearly visible. The black round object near the rear of the test section is the plastic bushing which was used to mount the model in the test section.

Test region.- The data in figure 6 indicated that near  $M = 1.28$  the  $20^\circ$ -wall-divergence case was the minimum wall divergence-angle setting at which a uniform center-line velocity distribution was present over a 3-inch test section length that was suitable for the wave reflection tests. For the wave reflection tests, therefore, the walls were set at  $20^\circ$  divergence. The selected test region extended from station  $8\frac{1}{8}$  to  $11\frac{1}{8}$ . Figure 7(b) is a schlieren photograph of the flow at  $M = 1.28$  with  $20^\circ$  of wall divergence, the condition at which the wave-reflection tests were made. The dashed vertical lines drawn in the downstream end of the test section indicate the location of the leading and trailing edges of the  $5^\circ$  wedge model. In the test region the maximum center-line Mach number variation was  $\pm 0.003$  at a Mach number of 1.28 with the walls diverged  $20^\circ$  (fig. 6(b)).

Vertical-velocity distributions in the test region at stations 8.5 and 10.5 are presented in figure 8 for  $20^\circ$  wall divergence and  $M = 1.283$ . This figure shows a Mach number variation of  $\pm 0.009$  at station 8.5 and a variation of  $\pm 0.004$  at station 10.5. The improved flow uniformity at station 10.5 is due to damping of the flow disturbances at the slotted walls between these two stations.

Effect of screen backing.- For the particular wall configuration tested, it was apparent from the data of figure 6 that the distance required to generate a uniform supersonic flow at a Mach number of 1.12 would be reduced considerably if the expansion-compression wave could be controlled. In an effort to exert some control on the magnitude of

CONFIDENTIAL

the initial flow expansion, a screen restriction, which spanned the width of the slotted wall and extended from  $x = 1.125$  inches to  $x = 4.125$  inches, was installed on the back surface of the slotted wall within the plenum tanks. This particular longitudinal location of the screen was the optimum location which resulted from numerous tests conducted with the restriction at various locations. Figure 9 presents the center-line Mach number distribution for this configuration at a Mach number of 1.12 with the walls parallel. The data for the basic wall configuration with no restriction are also presented for comparative purposes.

The addition of the screen reduced the initial-flow-expansion Mach number from approximately 1.121 to 1.080. This reduction in the initial flow expansion resulted in a flow generation pattern similar to that for the basic wall configuration at a Mach number of 1.20, with the net result that the restriction increased the damping characteristic of the wall so that a greater reduction in the cyclic-flow variations was effected in a shorter test-section length.

Effects of flow guides.- The results of the tests with the screen backing indicated that possibly the initial flow expansion could be controlled by a carefully designed flow guide. In order to evaluate the effectiveness of flow guide 1 in controlling the initial expansion, the slots were filled from  $x = 0$  to  $x = 1$  inch, which resulted in the formation of square end slots with a depth of 1 inch with the upstream slot origins located at  $x = 1$  inch. In comparing the flow-generation characteristics of the different flow-guide configurations presented in figure 10; it should be noted that the test-section minimum section was moved downstream for the flow-guides-removed case (slots filled from  $x = 0$  to  $x = 1$  inch). When compared with the flow-guides-removed configuration, flow guide 1 considerably reduced the magnitude and the sharpness of the expansion-compression wave. From these results, it was concluded that further improvements in the flow-generation characteristics might be obtained with a more gradually opening flow guide. Therefore, flow guide 2 was designed and tested.

A comparison of the flow-generation characteristics of flow guide 2 with those of flow guide 1 is also presented in figure 10, which indicates practically no difference in the generated flow. This is a surprising result, because the initial rate with which the slot depth increases with axial distance for flow guide 2 is only about 1/8 that for flow guide 1. From these results it would appear that a flow guide which increased the slot depth more slowly and perhaps a longer flow guide would be necessary in order to control further the initial flow expansion by varying the slot depth for this particular wall configuration.

## Shock-Wave Reflection

To aid in the evaluation of the experimental-wave-reflection data for the tunnel with 24-percent-open, deep, multislot walls, a discussion of the pressure variations adjacent to a wedge mounted in a non-viscous supersonic stream near a wall boundary (solid and porous) is presented. The sketch in figure 11 qualitatively indicates the trend of the static-pressure variations along a longitudinal line in a non-viscous supersonic flow field adjacent to a plain wedge mounted in a solid-wall wind tunnel. The static-pressure variations under these conditions would be seen as discontinuous static-pressure rises across the stream disturbances, and, within each flow region bounded by the disturbances, the static pressure would be constant. The static-pressure variations in a porous-wall tunnel should be similar to those in a solid-wall tunnel, except that the porous wall should reduce the rise in static pressure across the reflected shock. In fact, the porosity of the wall could be increased to the point where the incident shock would be reflected as an expansion, or for the optimum case a wall with the correct porosity would cancel the incident shock wave.

The experimental data of figure 12 show the static-pressure variations along three longitudinal lines located  $1/2$ ,  $3/4$ , and 1 inch from the tunnel center line at a free stream  $P/H$  corresponding to a Mach number of 1.278. The two shock strengths tested resulted in Mach number decrements  $\Delta M$  across the leading-edge shock of 0.07 and 0.12. The data for each longitudinal survey were plotted in a manner which allowed the various stream disturbances to be traced through the flow field. The vertical locations of these surveys in relation to the tunnel wall and model are presented in figure 13(a).

The experimental data of figure 12 show that a finite distance was required before the static-pressure rise across the initial shock wave reached an equilibrium condition. The apparent spreading of the initial shock wave was contrary to the preceding discussion for the nonviscous case and may be a result of the high static pressure in the leading-edge shock influencing the pressure at the static orifice through the static-tube boundary layer. This effect may be present in the reflection-test data at any point where the static orifice is in the vicinity of a sharp stream disturbance. As indicated in the discussion of the nonviscous case, the experimental data of figure 12 show that a constant-static-pressure region existed between the incident shock wave and the reflected disturbance. Whereas the nonviscous considerations predict a single reflected disturbance followed by a constant-pressure region, the experimental data show a mixed disturbance which consisted of a weak compression followed by a strong expansion and then a long region of compression. The initial compression-expansion disturbance may be explained by a close examination of the boundary conditions which exist at the point of intersection of the shock wave and the slotted wall. At this point

~~CONFIDENTIAL~~

a low-pressure area exists upstream of the incident shock and a high-pressure region exists downstream of the incident shock. Also, the schlieren photographs presented in figure 13(b) indicate the existence of a boundary layer on the slotted wall (although it should be pointed out that the boundary-layer thickness indicated in the schlieren photographs includes the combined effects of the glass-side-wall and the multislotted-wall boundary layers in the corners of the test section). Under these conditions, the high pressure downstream of the incident shock wave could be transmitted forward through the wall boundary layer or within the wall slots and cause an increase in the boundary-layer growth forward of the shock-boundary-layer intersection. The abnormal boundary-layer growth would result in the formation of a compression wave which would account for the compression wave seen in the experimental data. The reflected expansion shown in the experimental data could be a result of the incident shock wave impinging upon the thickened wall boundary layer. The high pressure behind the shock would tend to turn the wall boundary layer at a sharp angle toward and out through the slots, and thereby cause an expansion in the flow outside the boundary layer.

The compression that followed the expansion extended rearward at least as far as the point where it intersected the reflection from the model of the initial compression-expansion disturbance. This occurred at about  $x = 2\frac{3}{8}$  inches for the survey at 1 inch from the tunnel center line shown in figure 12(a). The compression region could be generated by three sources, namely, the forward portion of the model, the shock-wave boundary-layer interaction, or the slotted wall adjacent to the compression region. The fairly constant pressure field between the leading-edge shock and the reflected disturbance eliminates the model as a source of the compression, and although interaction of the incident shock wave and the wall boundary layer could produce a compression originating near the shock-boundary-layer intersection, the long observed compression region could not be generated by such a localized disturbance. Therefore, the compression was probably due to a progressively decreasing effective wall porosity in the region behind the shock-boundary-layer intersection.

From the analysis of the wave-reflection data, it may be concluded that an investigation of the causes of the mixed reflection will require some means of separating the effects of forward pressure travel through the boundary layer and through the wall itself. The general compression region created by the deep slotted wall indicated that this particular wall configuration for the conditions tested was undesirable as a means of reducing boundary-reflected disturbances.

Subsonic Operation of Test Section With  
Deep Multislotted Walls

A close examination of figure 6 for the  $M = 0.8$  case at wall divergence angles of  $0'$ ,  $20'$ , and  $40'$  shows that the flow near the diffuser entrance could be accelerated or decelerated without affecting the center-line velocity distribution in the test section. The data of figure 14 are presented in order to explain these velocity changes in the subsonic case and to obtain some idea of the physical conditions which resulted in the changes in the center-line velocity near the diffuser entrance.

In order to have a constant subsonic center-line Mach number distribution for parallel walls with or without suction in any partly open test section, it is necessary that a sufficient mass of air be removed through the openings to compensate for the growth of the boundary layer on the walls.

From this consideration, the absence of a velocity gradient in the forward portion of the test section for the subsonic no-suction condition (fig. 14) indicated that air was taken from the tunnel main stream into the plenum tanks. In this no-suction case the air entering the tanks had to be returned to the tunnel main stream in order to obey the continuity-of-mass law. The region wherein this air was returned to the tunnel stream is the accelerated-flow region near the diffuser. In this area the inflow of low-velocity air from the plenum tanks restricted the main stream and resulted in a flow acceleration. From these observations, it was concluded that for subsonic operation of a slotted test section with parallel walls and without suction a flow acceleration will exist in the region near the diffuser.

The constant center-line Mach number distribution for the suction case (fig. 14) indicated that the correct mass of air was removed in order to compensate for the growth of the slotted-wall boundary layer. Removing the air through the separate source of suction prevented the inflow of air into the tunnel near the diffuser entrance which resulted in a constant velocity in the rear of the test section. It should be noted that near the diffuser entrance it was possible for an excessive mass of air to be forced into the plenum tanks from the tunnel air stream if the static pressure in the diffuser was higher than the plenum-tank static pressure. Under these conditions the mass flow in the tunnel stream decreases at a greater rate than is necessary to compensate for the wall-boundary-layer growth. The decrease in the tunnel mass flow would result in a decrease in the tunnel stream velocity in the region near the diffuser entrance. This effect can be seen at the rear of the test section in figure 6(c) at  $M = 0.824$ . The preceding discussion has shown that the velocity distribution near the diffuser entrance is a function of the mass of air removed by suction in the case of the present

slotted test section. This same result would be expected for any partly open test section, as for instance in a perforated test section.

In order to obtain the constant center-line Mach number distribution, the subsonic speed control of this slotted-wall tunnel resolved into two separate operations. The first operation consisted of setting the correct Mach number at a point in the forward portion of the test region (approximately  $x = 8$  inches). The primary control of the Mach number at this point was the plenum-tank pressure which was determined by the speed of the suction equipment. The second operation was to set the velocity near the diffuser entrance equal to the velocity at  $x = 8$  inches. This velocity was controlled by the speed of the tunnel main-drive compressor. This manner of operation results in a maximum usable subsonic test-section length.

#### Outflow Requirements

From power considerations for a slotted- or porous-wall wind tunnel, the suction flow or outflow required to generate a certain Mach number would be of interest to the wind-tunnel designer. Therefore, during the course of testing the 24-percent-open, deep, multislot wall, the outflow was determined for the Mach number range from  $M = 0.8$  to  $1.3$  and for wall-divergence angles of  $0'$ ,  $20'$ , and  $40'$ . The data obtained from these tests are presented in figure 15. The total slotted-wall area and average tunnel-throat area were  $79.22$  and  $8.93$  square inches, respectively.

As emphasized in the tunnel subsonic operation section, there existed numerous combinations of tunnel main-drive and suction settings which would result in the generation of identical Mach numbers in the forward portion of the test region. For each power combination, the subsonic velocity distribution near the diffuser entrance and the mass of the suction outflow changes, but for each Mach number, one particular power combination will result in a constant velocity distribution near the diffuser. In this investigation the power combination which produced a constant velocity distribution was used as a basis for the power settings for the suction-outflow measurements at the subsonic speeds. It should be pointed out that for the subsonic speeds a comparison between the suction-outflow data for two configurations would not be valid if the velocity distributions near the diffuser entrance were not comparable.

The data of figure 15 show that below Mach number 1 for all divergence angles, the slopes of the outflow curves decrease and approach a constant outflow condition. Generally, above Mach number 1 the required outflow was increased with increasing Mach number. This effect would be expected at the supersonic speeds because the flow-expansion requirements increase with Mach number.

The effect of increasing the wall-divergence angles was to decrease the outflow and the suction power required to generate a given Mach number. This effect may be explained by the fact that the mass to be removed in order to compensate for the slotted-wall boundary layer was decreased because the wall divergence tended to compensate for the wall boundary layer. An additional factor at supersonic speeds is the fact that if the walls are diverged beyond the angle required for boundary-layer compensation, the divergence itself will permit some flow expansion, thus reducing the required suction flow.

### CONCLUSIONS

The wave-reflection and flow-generation characteristics of a two-dimensional wind tunnel with 24-percent-open, deep, multislot walls were studied. The results of these tests lead to the following conclusions:

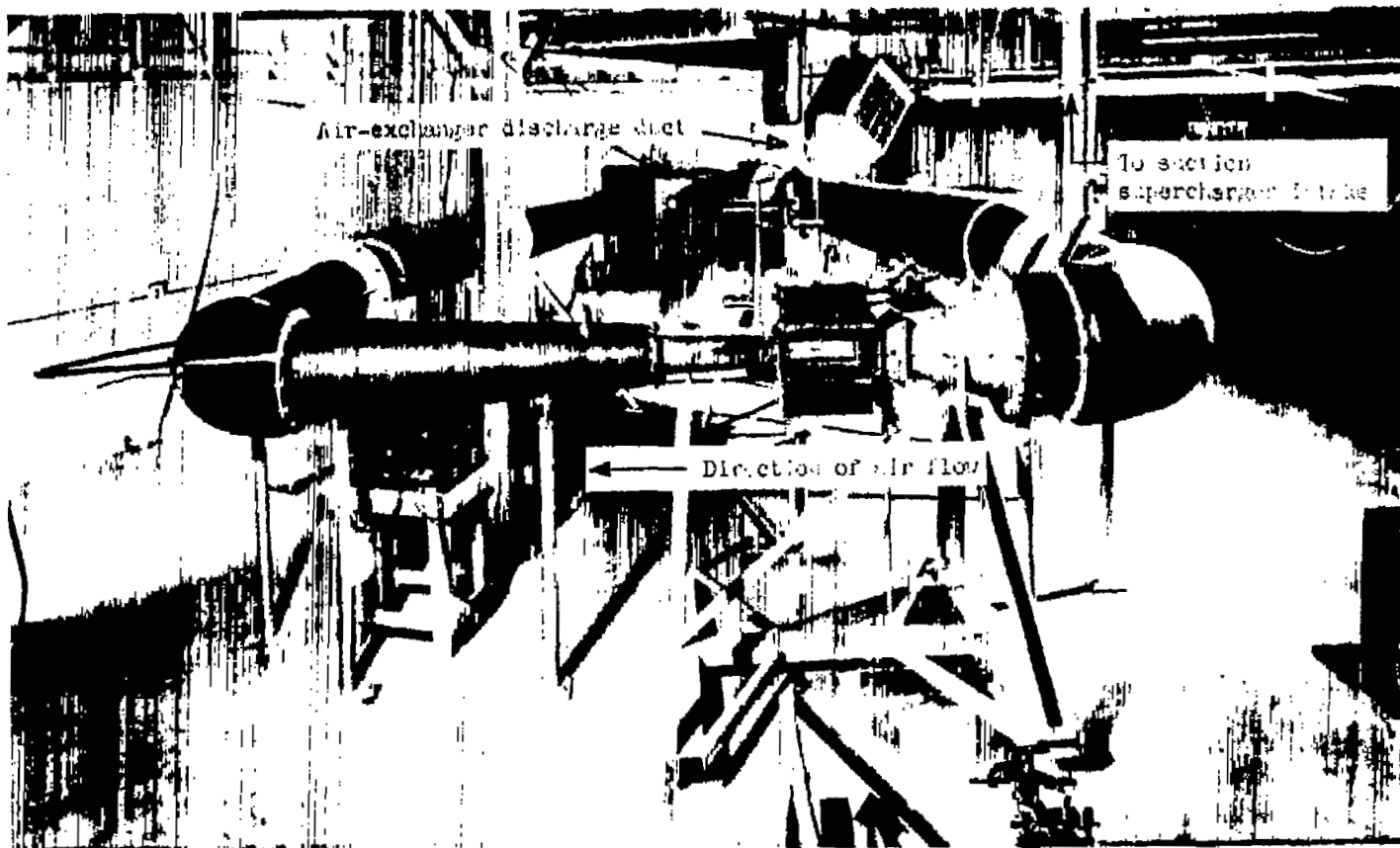
1. At a free-stream Mach number of 1.278 and a wall-divergence angle of 20', the incident shock wave was reflected from the wall as a mixed disturbance which consisted of a weak compression followed by a strong expansion wave and a long compression region. Because of this mixed reflection, the 24-percent-open, deep, multislot wall is unsatisfactory as a means of reducing boundary-reflected disturbances.
2. Future shock-wave-reflection investigations should include means of separating the effects of the pressure travel forward through the wall boundary layer and within the wall itself.
3. Generally except for the zero-wall-divergence case at the high Mach numbers, for Mach numbers from 0.80 to 1.28 at wall-divergence angles of 0', 20', and 40', the center-line Mach number variations in the flow generated by the 24-percent-open, deep, slotted wall in a test section length of  $2\frac{2}{3}$  tunnel heights do not exceed  $\pm 0.005$  in Mach number over a test region length of 1 tunnel height. For the zero-wall-divergence case at  $M = 1.32$ , the center-line Mach number variations were within  $\pm 0.01$ .
4. In this slotted-wall wind tunnel equipped with suction at subsonic speeds, the velocity distribution near the diffuser entrance is a function of the mass of air removed by suction.

5. Slight wall divergence improves the center-line velocity distribution near  $M = 1.3$  and furthermore wall divergence reduces the suction power required to generate a given Mach number.

Langley Aeronautical Laboratory,  
National Advisory Committee for Aeronautics,  
Langley Field, Va., October 7, 1953.

#### REFERENCES

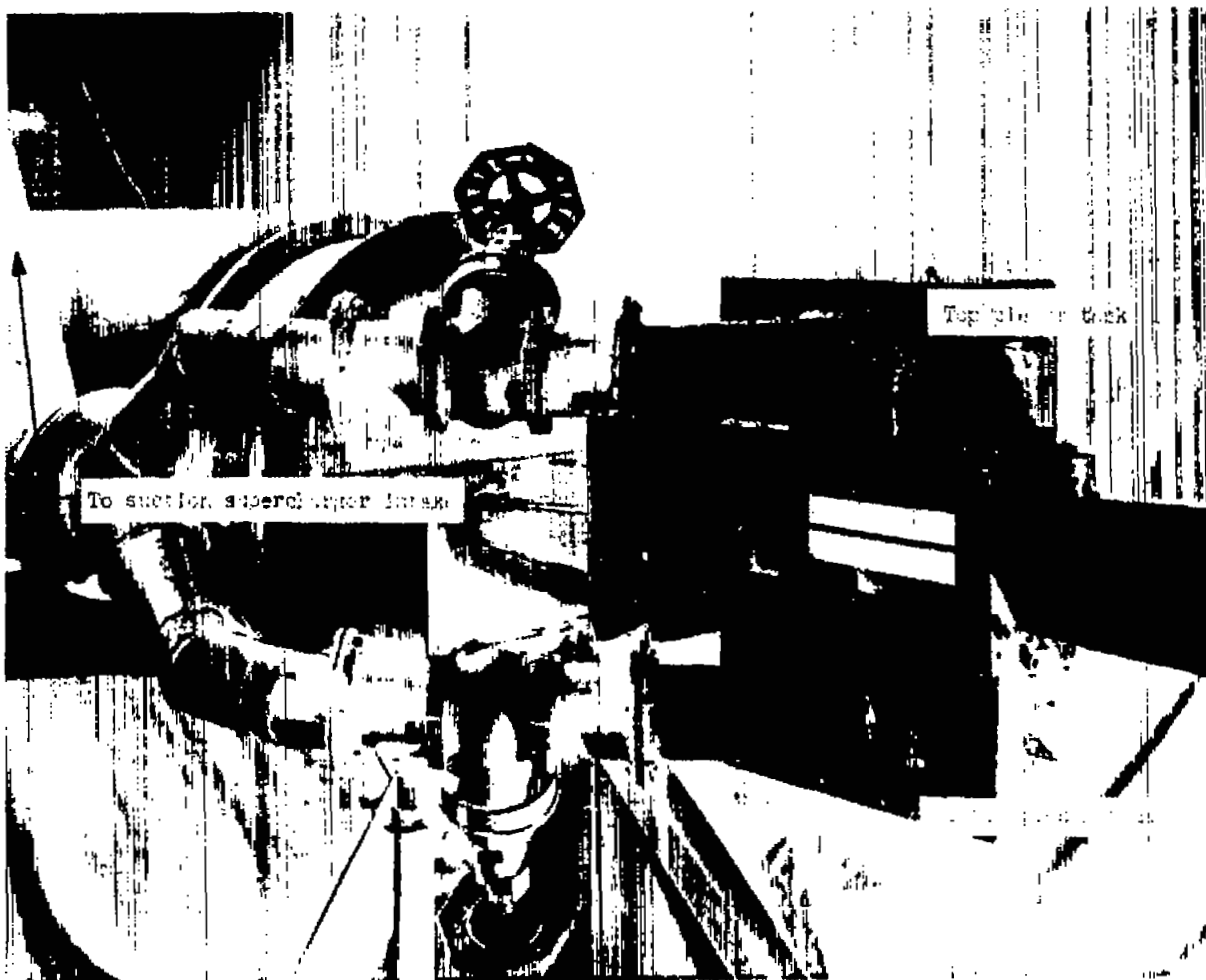
1. Ritchie, Virgil S., and Pearson, Albin O.: Calibration of the Slotted Test Section of the Langley 8-Foot Transonic Tunnel and Preliminary Experimental Investigation of Boundary-Reflected Disturbances. NACA RM L51K14, 1952.
2. Davis, Don D., Jr., and Wood, George P.: Preliminary Investigation of Reflections of Oblique Waves From a Porous Wall. NACA RM L50G19a, 1950.
3. Nelson, William J., and Bloetscher, Frederick: Preliminary Investigation of Porous Walls As a Means of Reducing Tunnel Boundary Effects at Low-Supersonic Mach Numbers. NACA RM L50D27, 1950.



(a) General view.

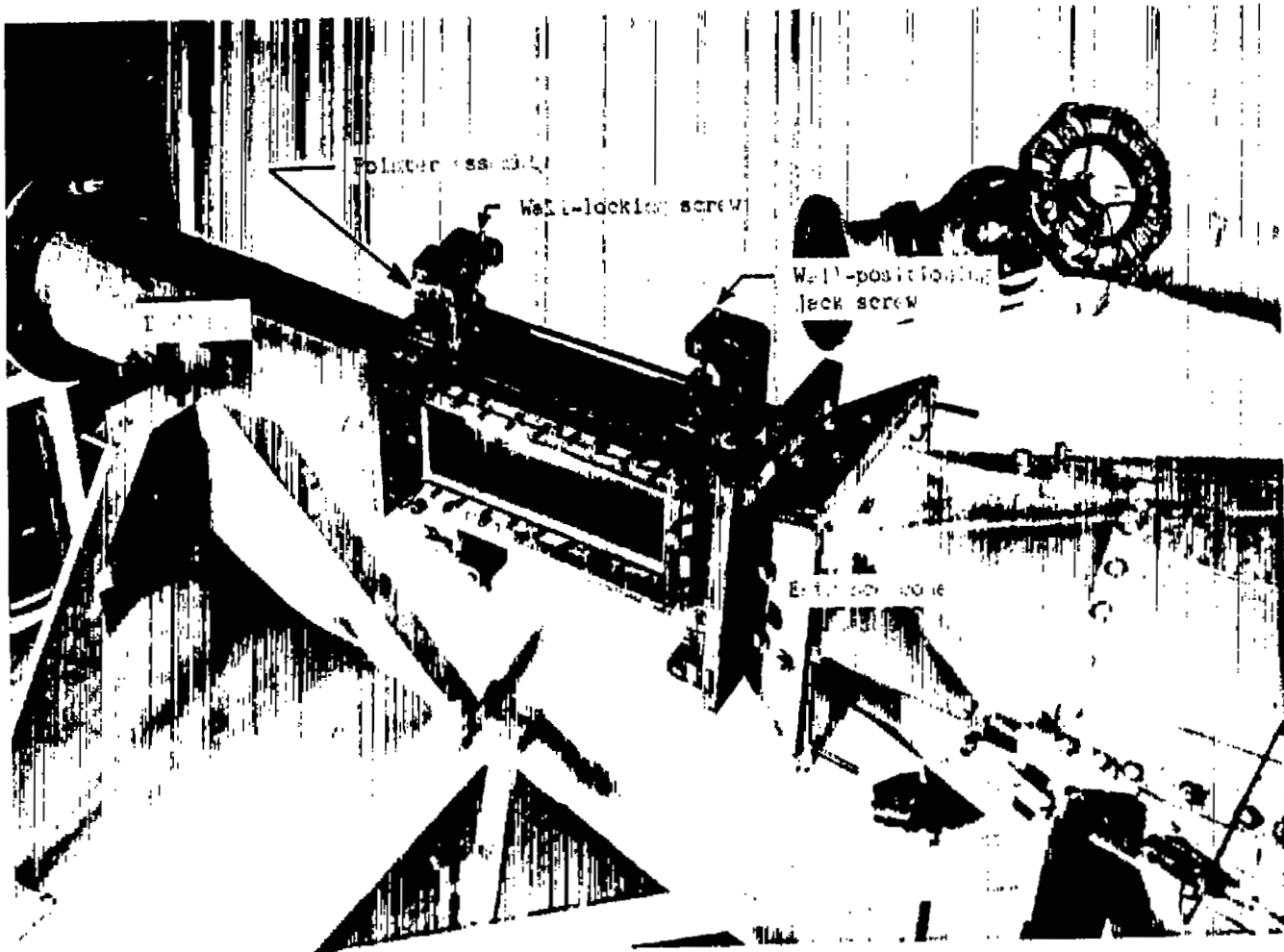
L-73103.1

Figure 1.- Photographs of the transonic flow apparatus and auxiliary equipment.



(b) Details of the plenum tanks and ducting. L-73105.1

Figure 1.- Continued.



(c) Details of the removable test section  
and wall-diverging mechanism.

L-73104.1

Figure 1.- Concluded.

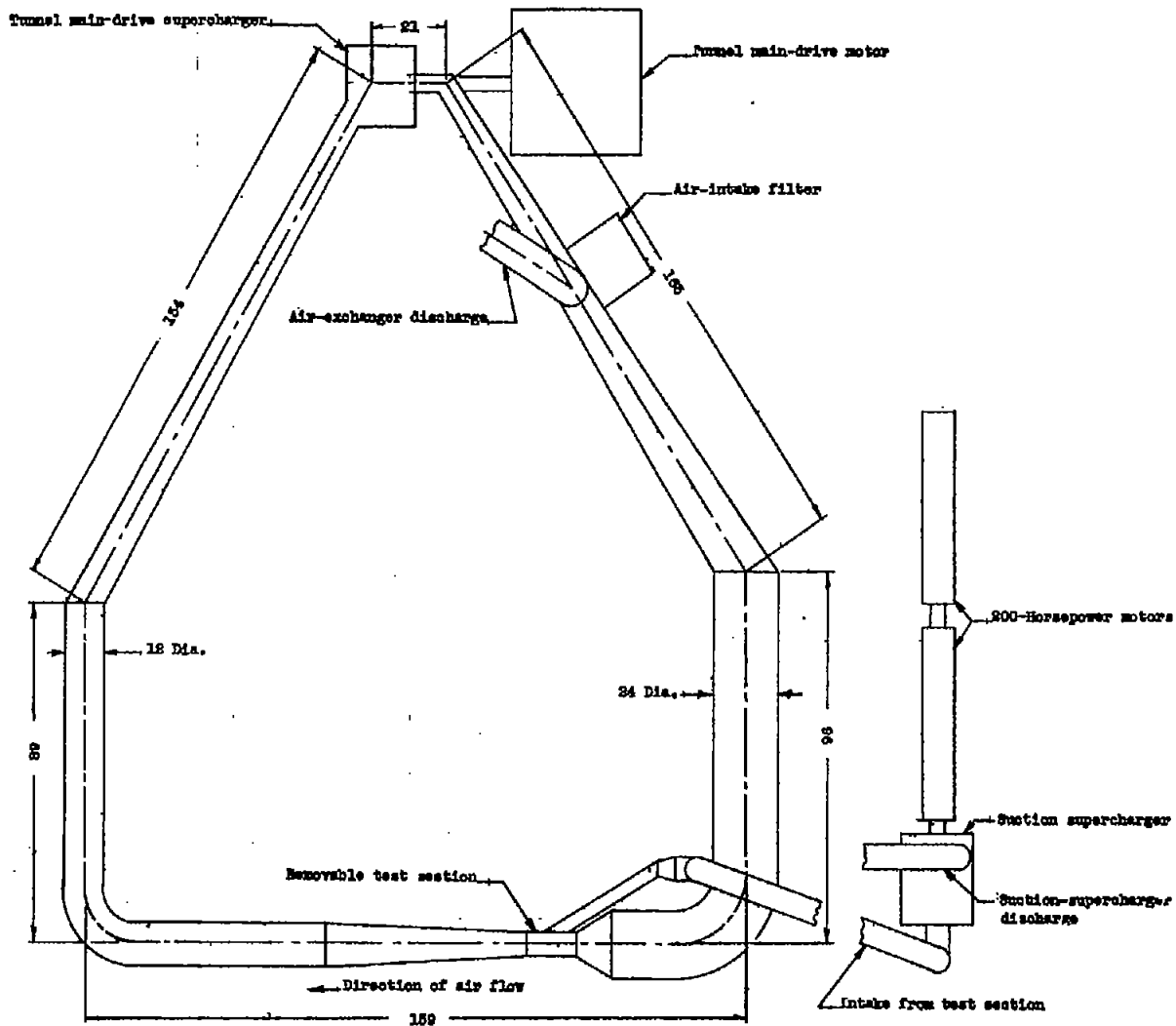
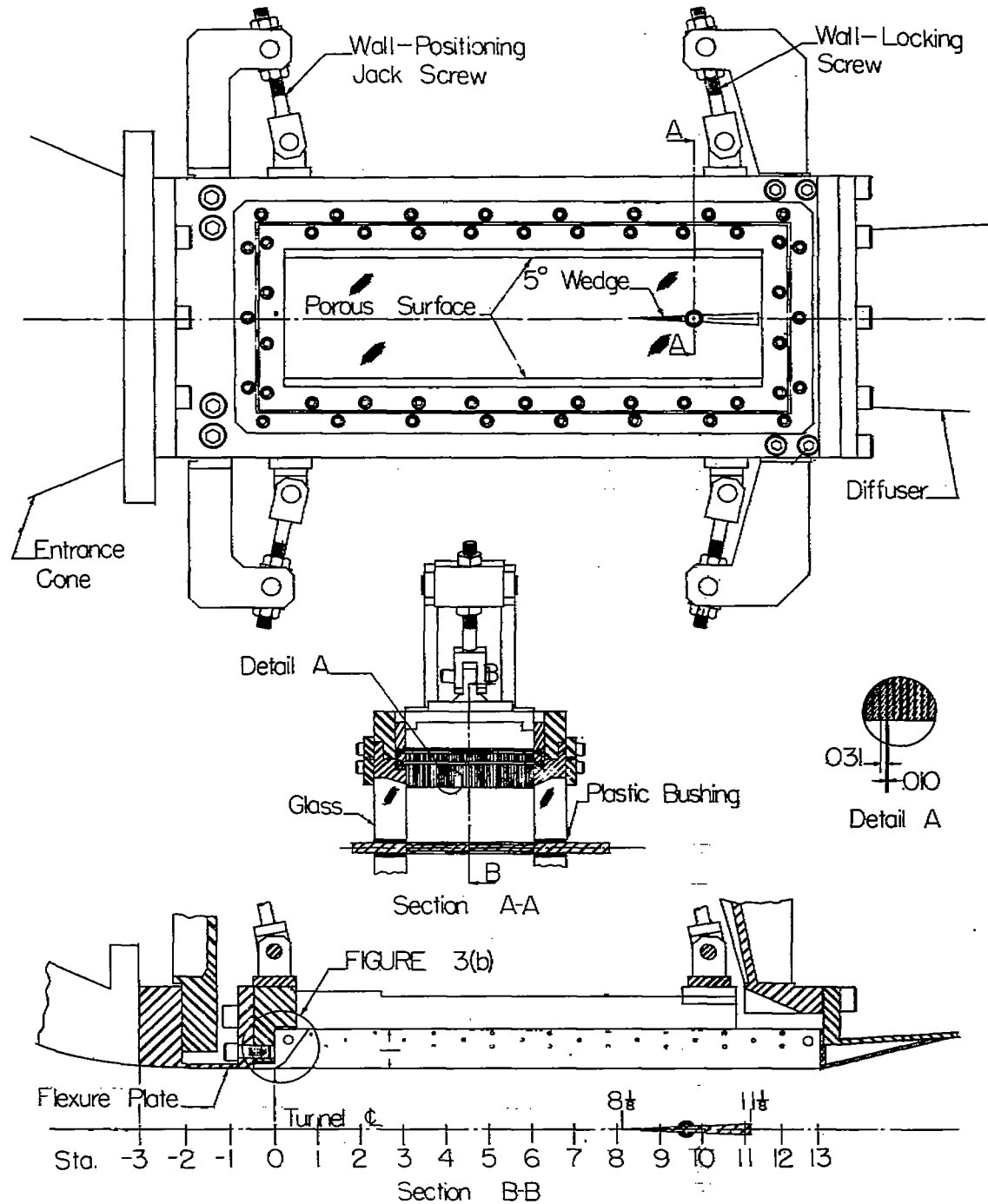


Figure 2.- Schematic layout of the transonic flow apparatus and auxiliary equipment. All dimensions are in inches.

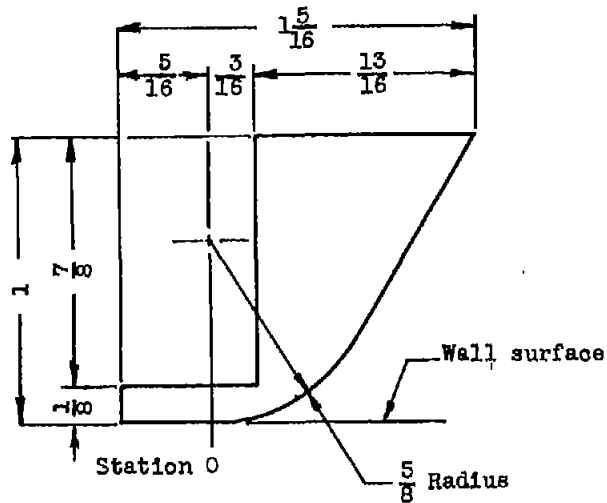


(a) Construction details.

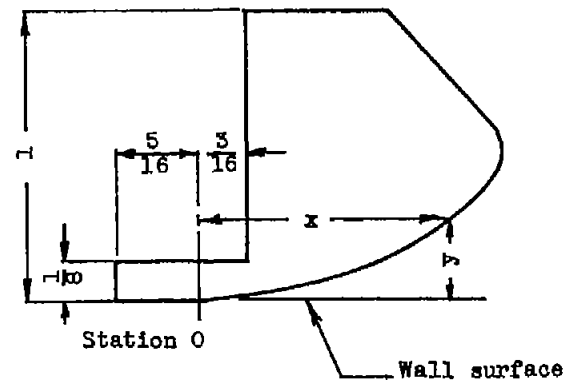
Figure 3.- Details and dimensions of test section with 24-percent-open, deep, multislotted wall. All dimensions are in inches.

Table of ordinates  
Flow Guide 2

x	y
0	0
0.100	0.0036
0.200	0.0125
0.300	0.0283
0.400	0.0500
0.500	0.0786
0.600	0.1131
0.700	0.1540
0.800	0.2008
0.900	0.2550
1.000	0.3240
1.060	0.4000
1.100	0.5000
1.075	0.6000
0.700	1.0000



Flow Guide 1



Flow Guide 2

(b) Details of flow guides 1 and 2.

Figure 3.- Concluded.

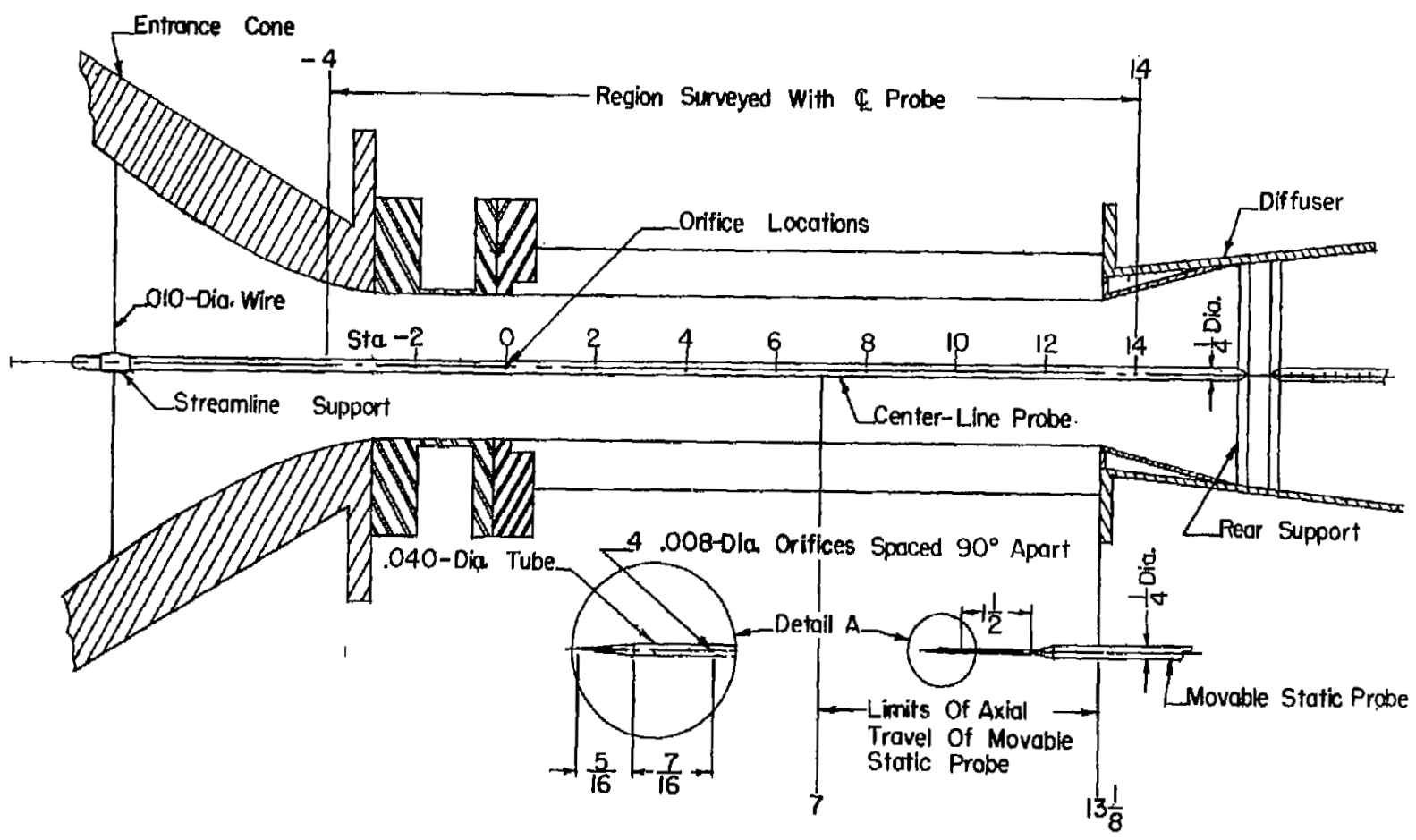


Figure 4.- Dimensions and details of the center-line probe and movable static probe. All dimensions are in inches.

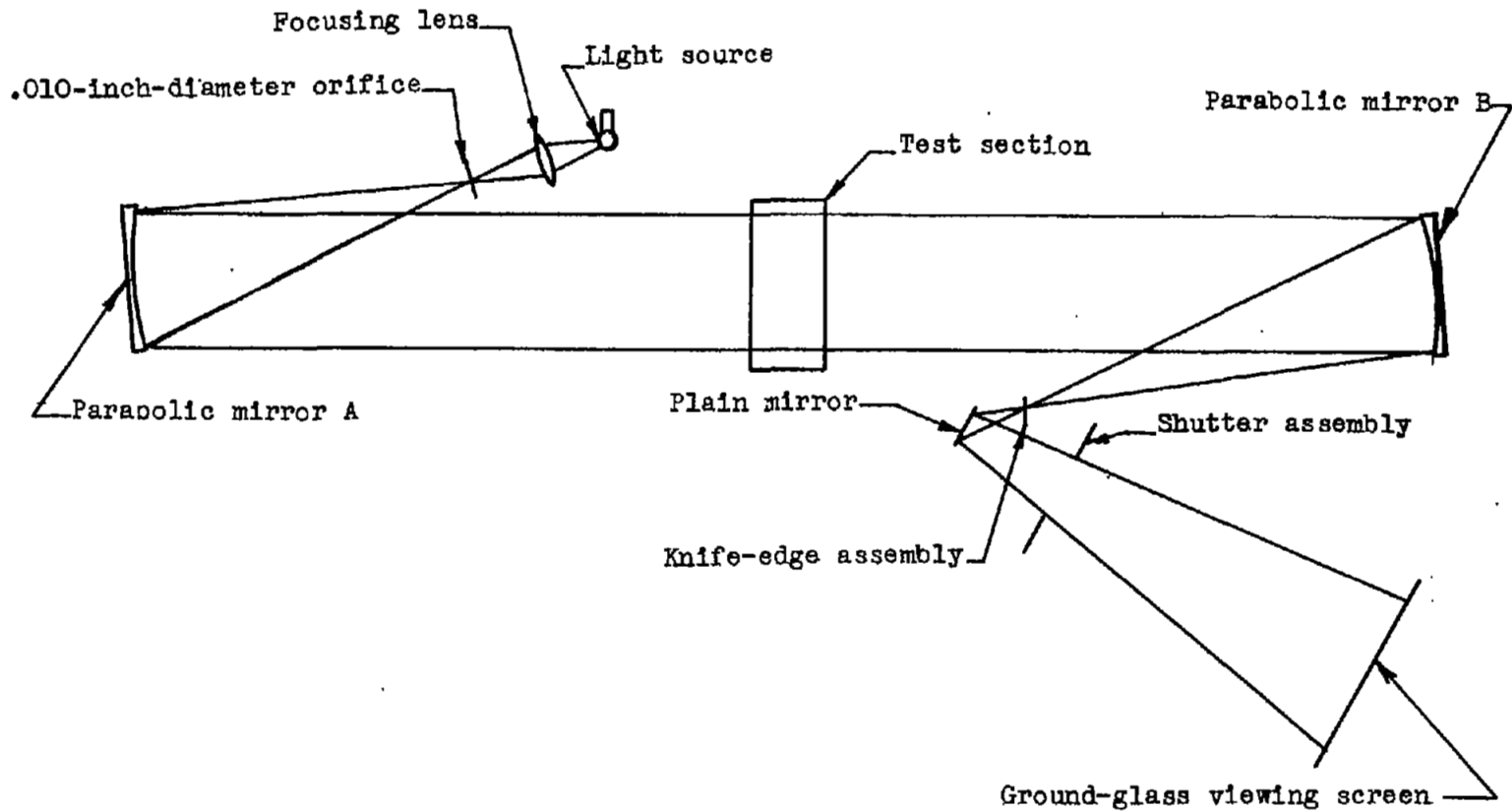
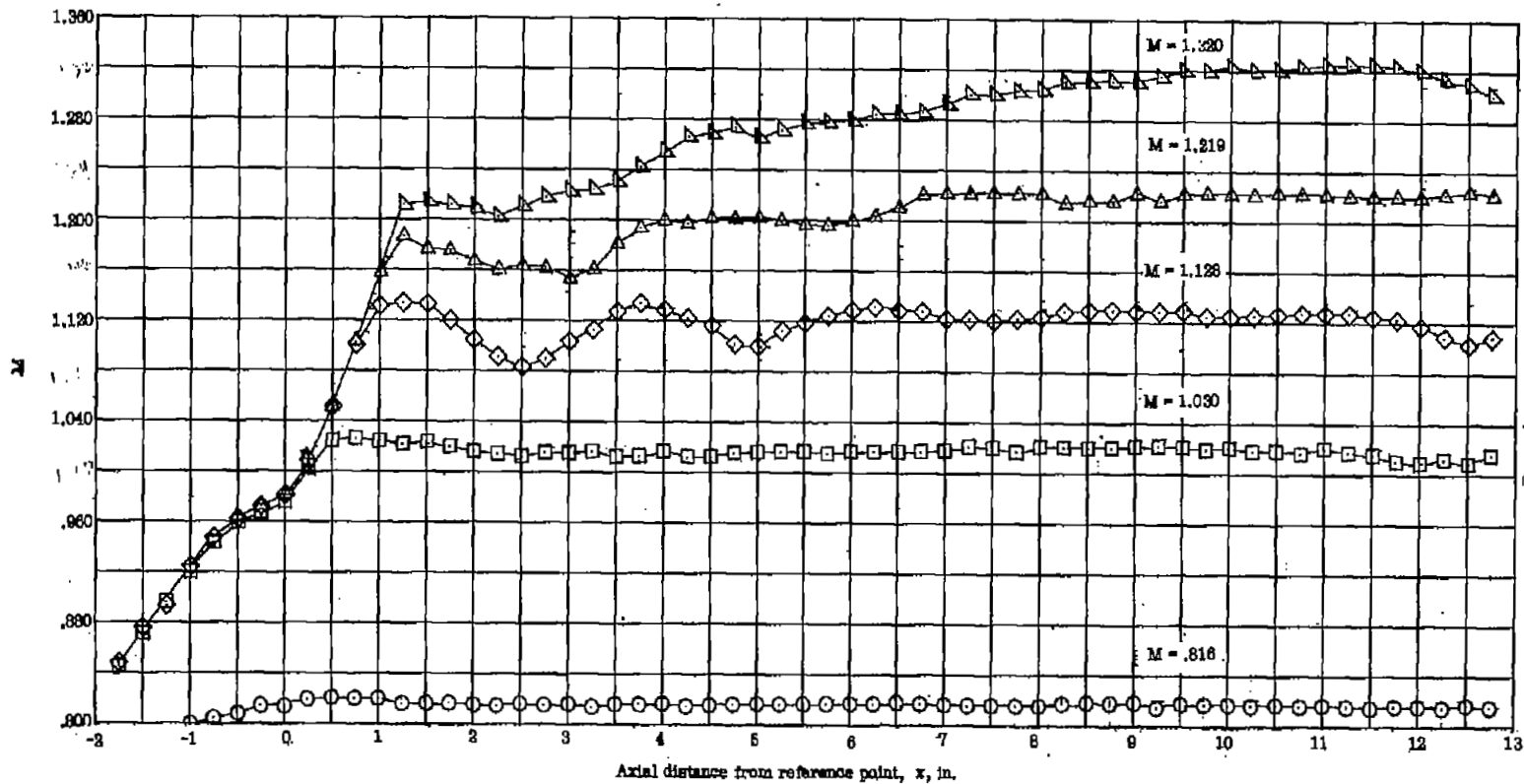
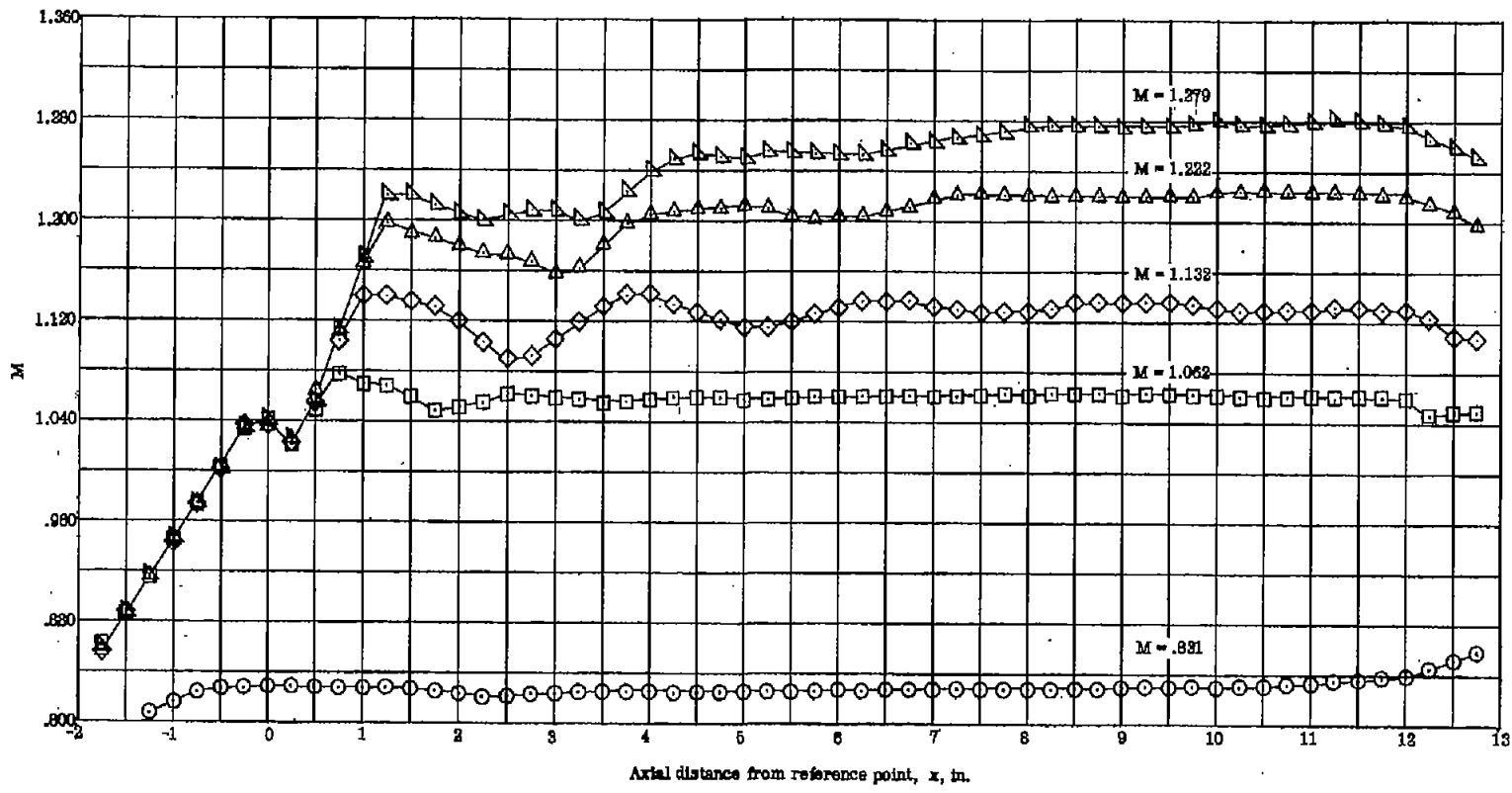


Figure 5.- Schematic of the schlieren system.



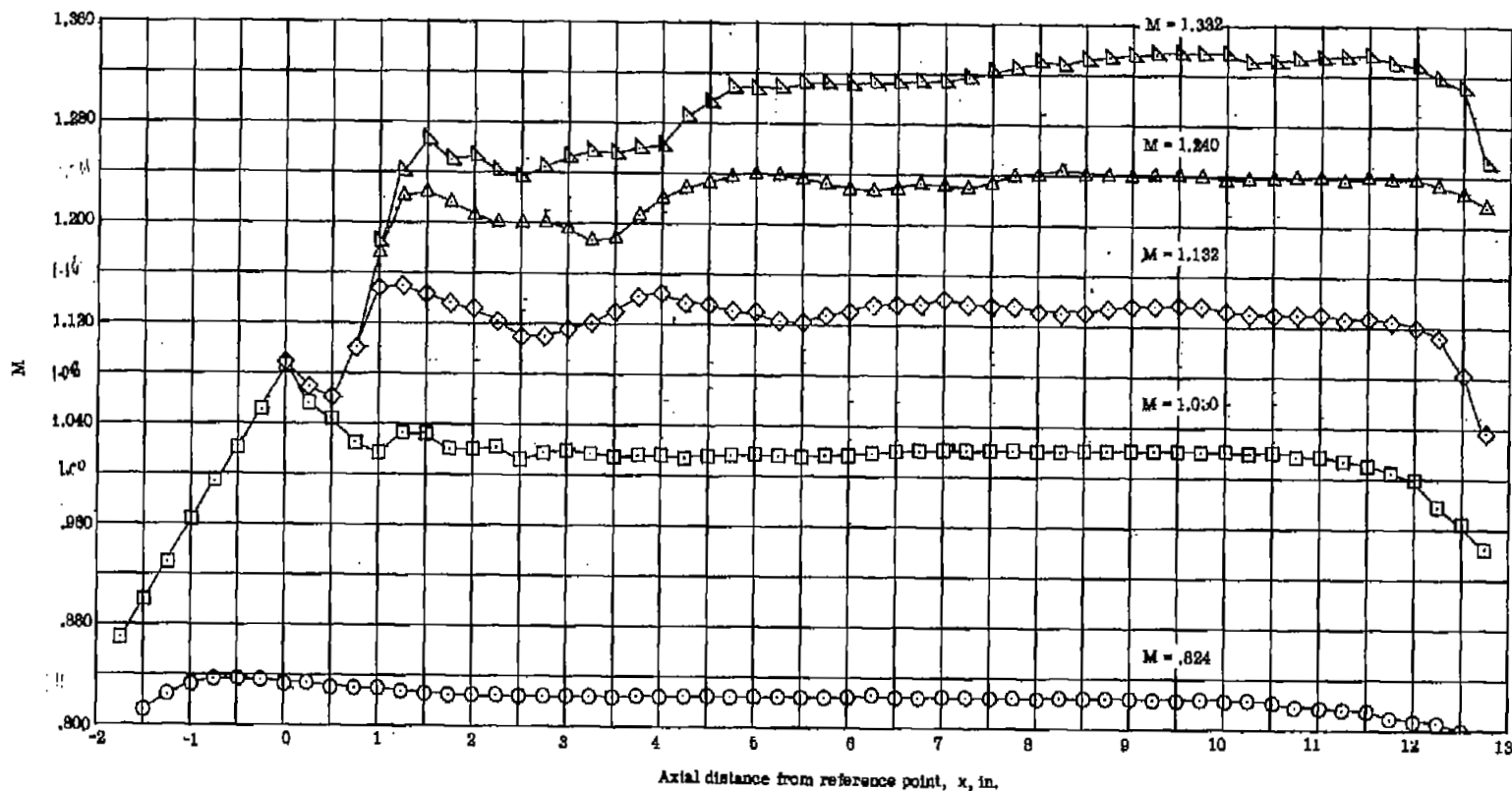
(a) Wall divergence angle, 0'.

Figure 6.- Center-line Mach number distributions for three tunnel-wall divergence angles. Basic wall configuration.



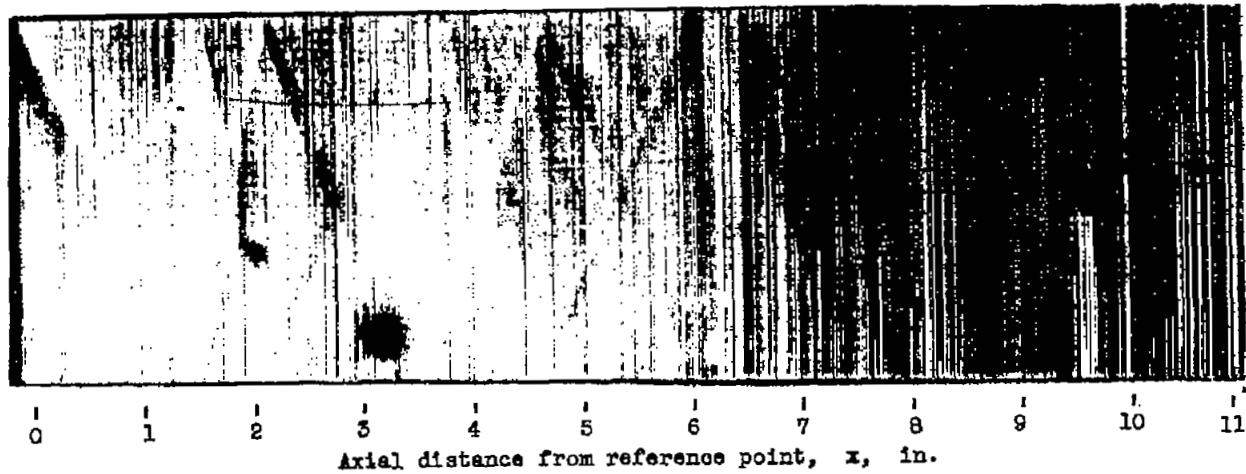
(b) Wall divergence angle, 20'.

Figure 6.- Continued.

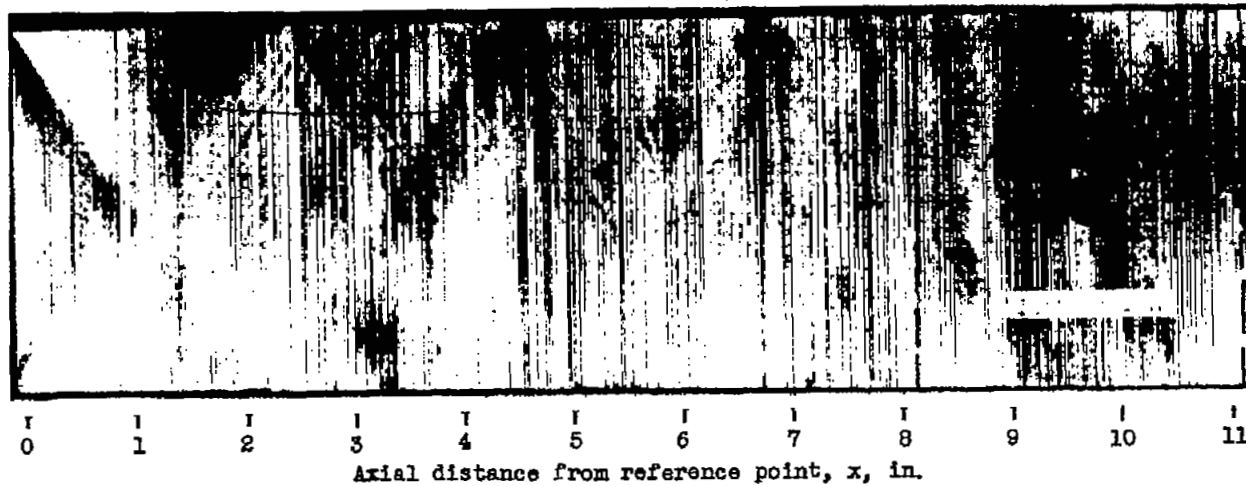


(c) Wall divergence angle, 40'.

Figure 6.- Concluded.



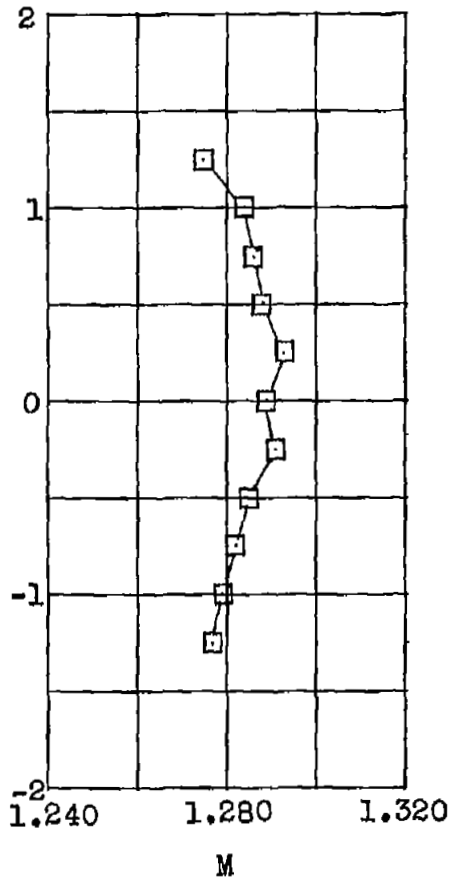
(a) Test-section Mach number, 1.12.



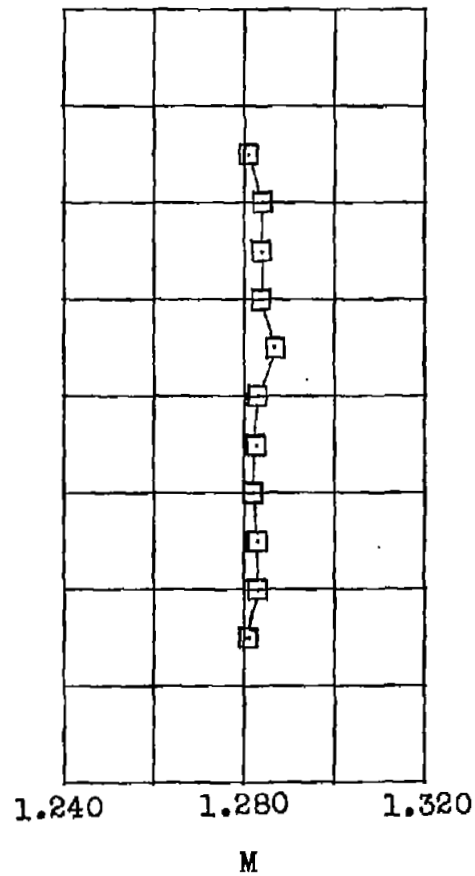
(b) Test-section Mach number, 1.278.

Figure 7.- Schlieren photographs of the empty tunnel at two test-section Mach numbers. Wall divergence angle,  $20^\circ$ ; basic wall configuration.

Vertical distance from tunnel center line,  $z$ , in.



Station 8.5



Station 10.5

Figure 8.- Vertical Mach number distributions at two longitudinal positions.  
Wall divergence angle,  $20'$ ;  $M = 1.283$ ; basic wall configuration.

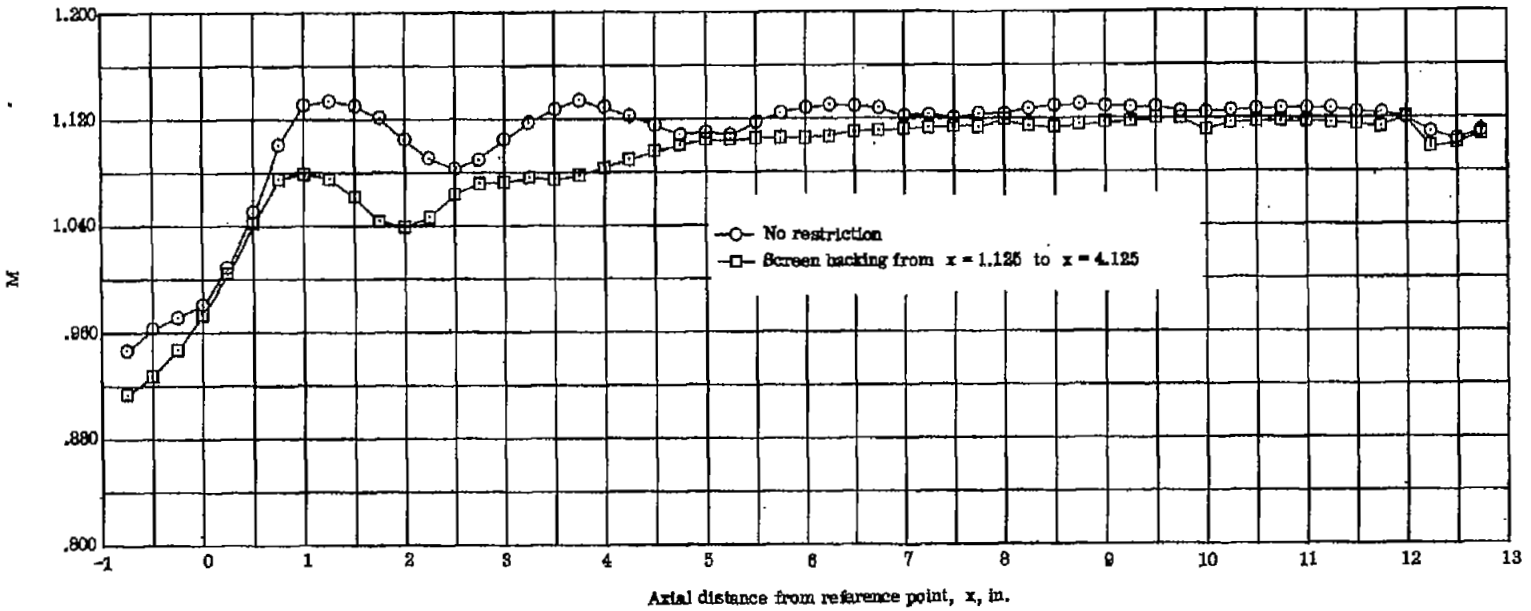


Figure 9.- Effects on center-line Mach number distribution of installing a screen backing from  $x = 1.125$  inches to  $x = 4.125$  inches. Wall divergence angle,  $0'$ ;  $M = 1.12$ ; basic wall configuration.

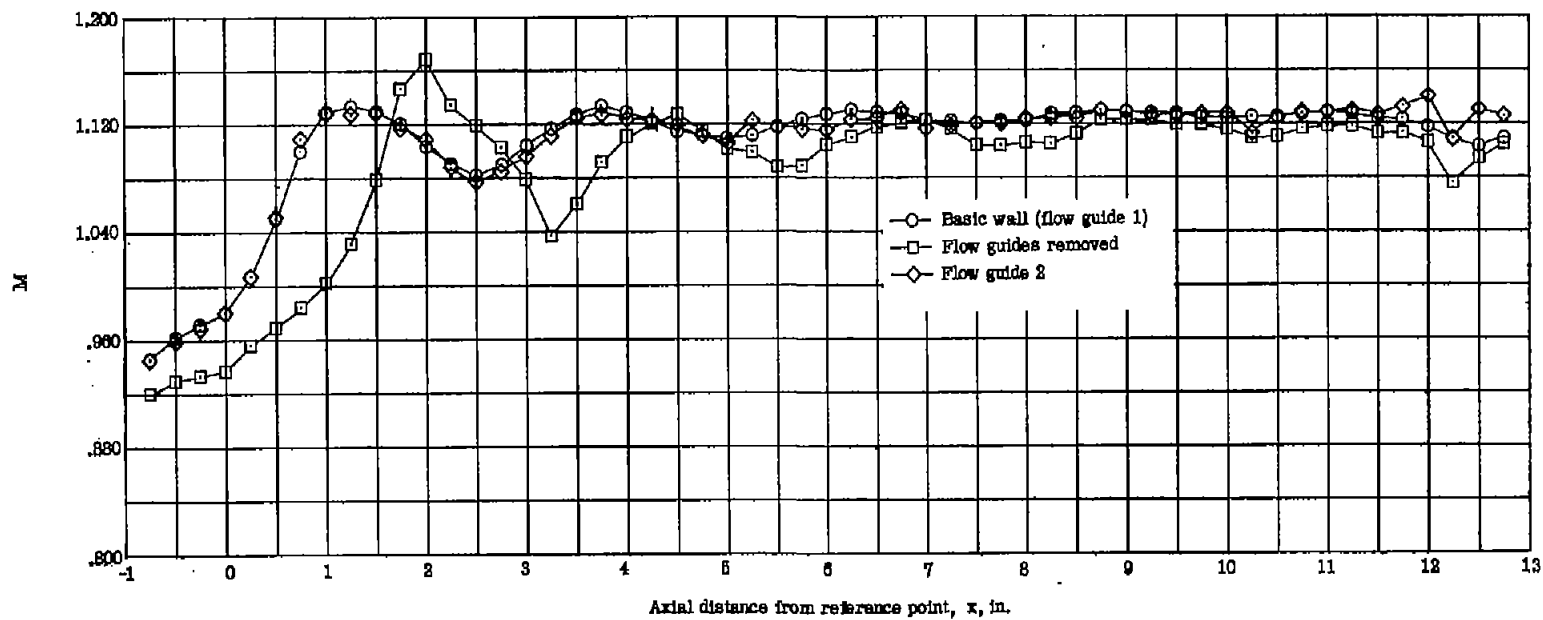


Figure 10.- Center-line Mach number distribution generated by flow guides 1 and 2 compared with the flow generated with flow guides removed. Wall divergence angle, 0'; M = 1.12.

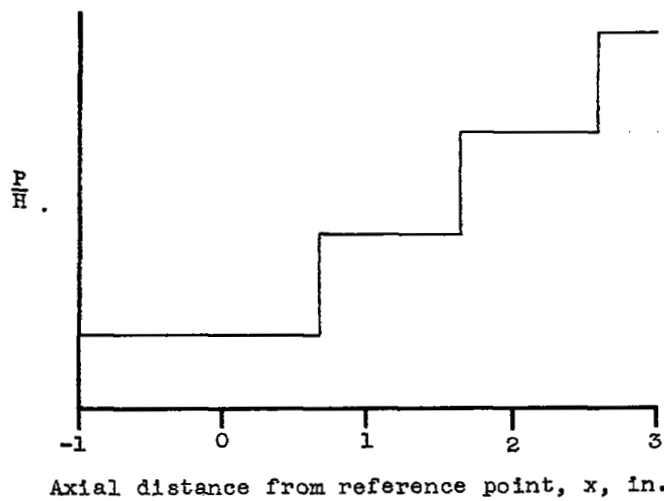
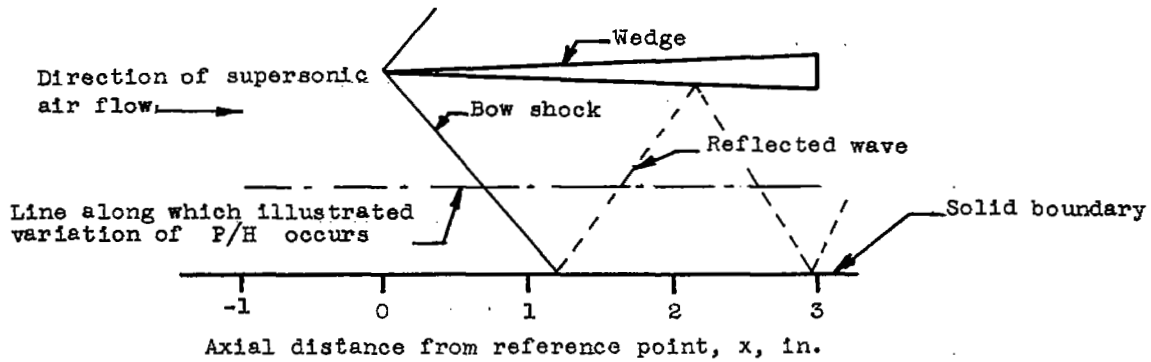


Figure 11.- Static-pressure variations in a flow field adjacent to a wedge mounted in a nonviscous supersonic flow in a solid-wall wind tunnel.

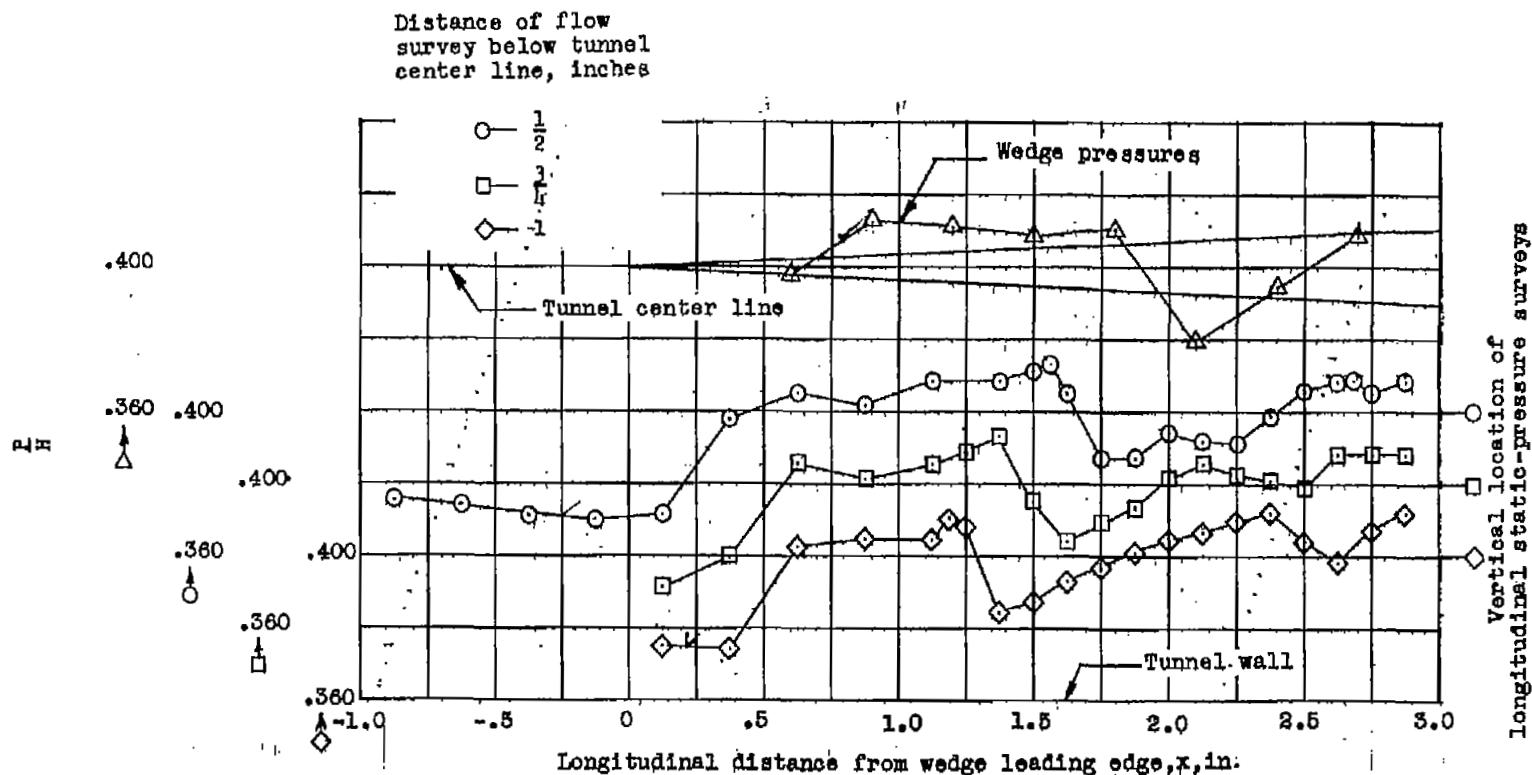
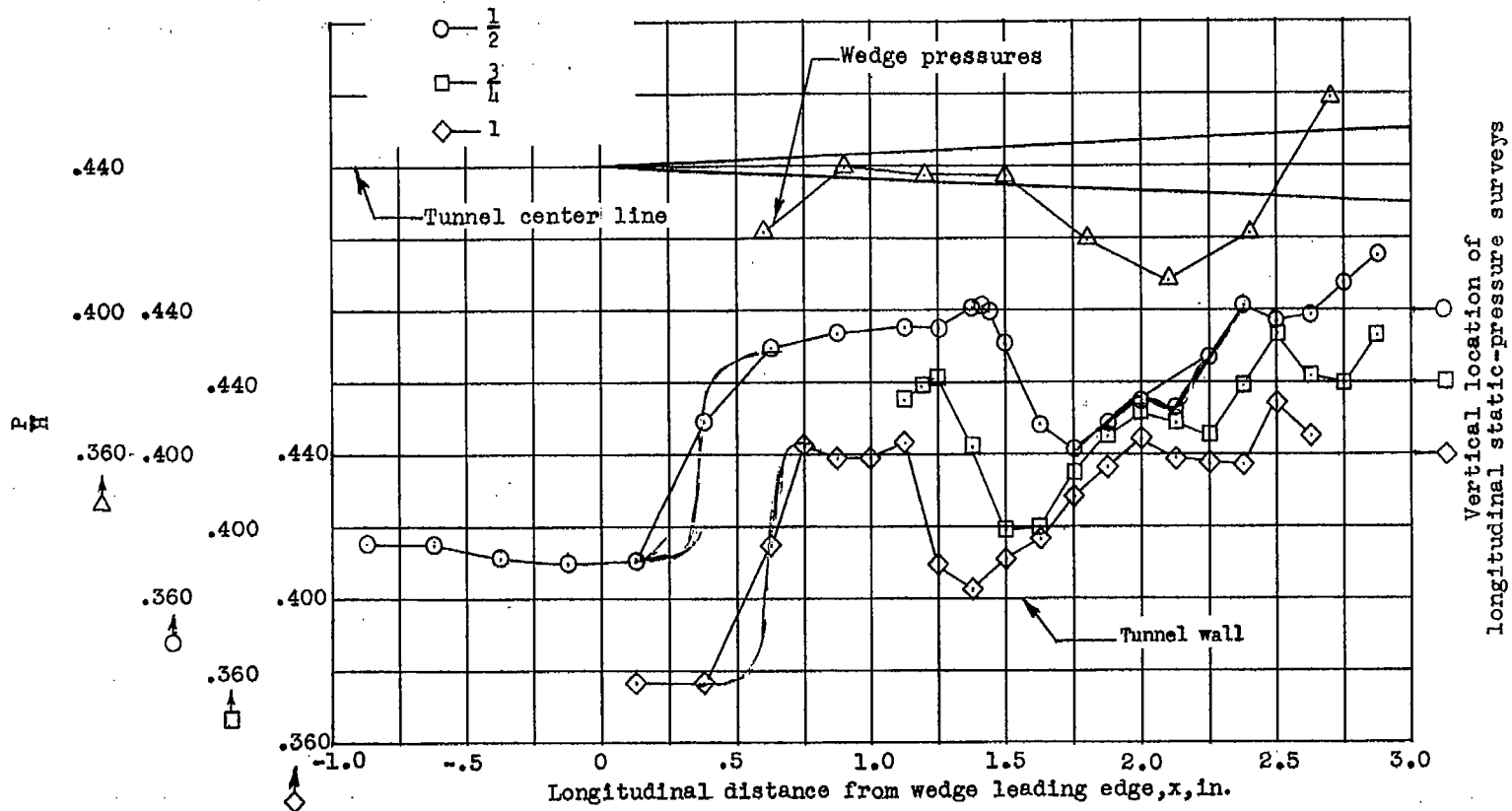
(a)  $\Delta M = 0.07$ .

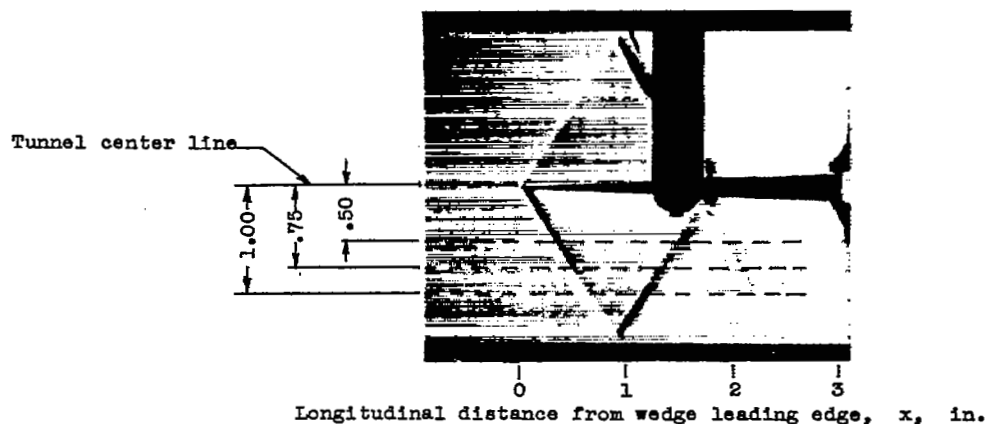
Figure 12.- Experimental static-pressure surveys for two initial shock-wave strengths in the flow field adjacent to a  $5^\circ$  wedge mounted in a wind tunnel with 24-percent-open, deep, multislot walls at a free-stream  $P/H$  that corresponds to a Mach number of 1.278. Wall divergence angle,  $20'$ ; basic wall configuration.

Distance of flow survey below tunnel center line, inches

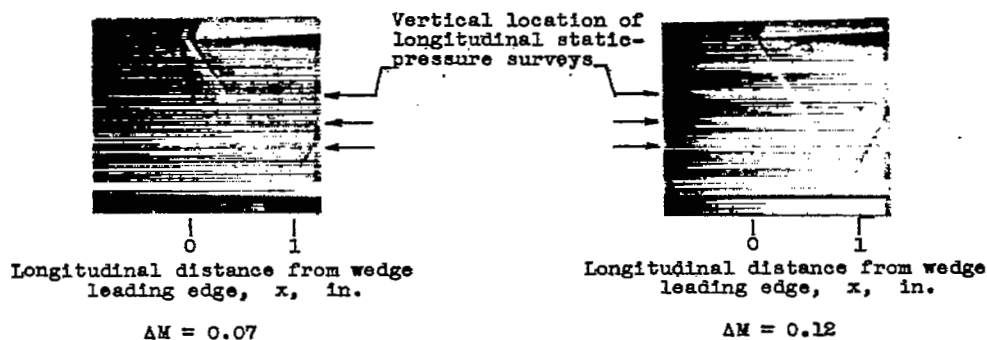


(b)  $\Delta M = 0.12$ .

Figure 12.- Concluded.



(a) General model installation details and the vertical locations of the longitudinal static-pressure surveys. All dimensions are in inches.



(b) Views of the incident shock wave and reflection with a boundary layer on the tunnel wall for two shock strengths.

Figure 13.- Schlieren photographs of  $5^\circ$  wedge model mounted in test section. Wall divergence angle,  $20'$ ; free-stream  $P/H = 0.372$ ; basic wall configuration.

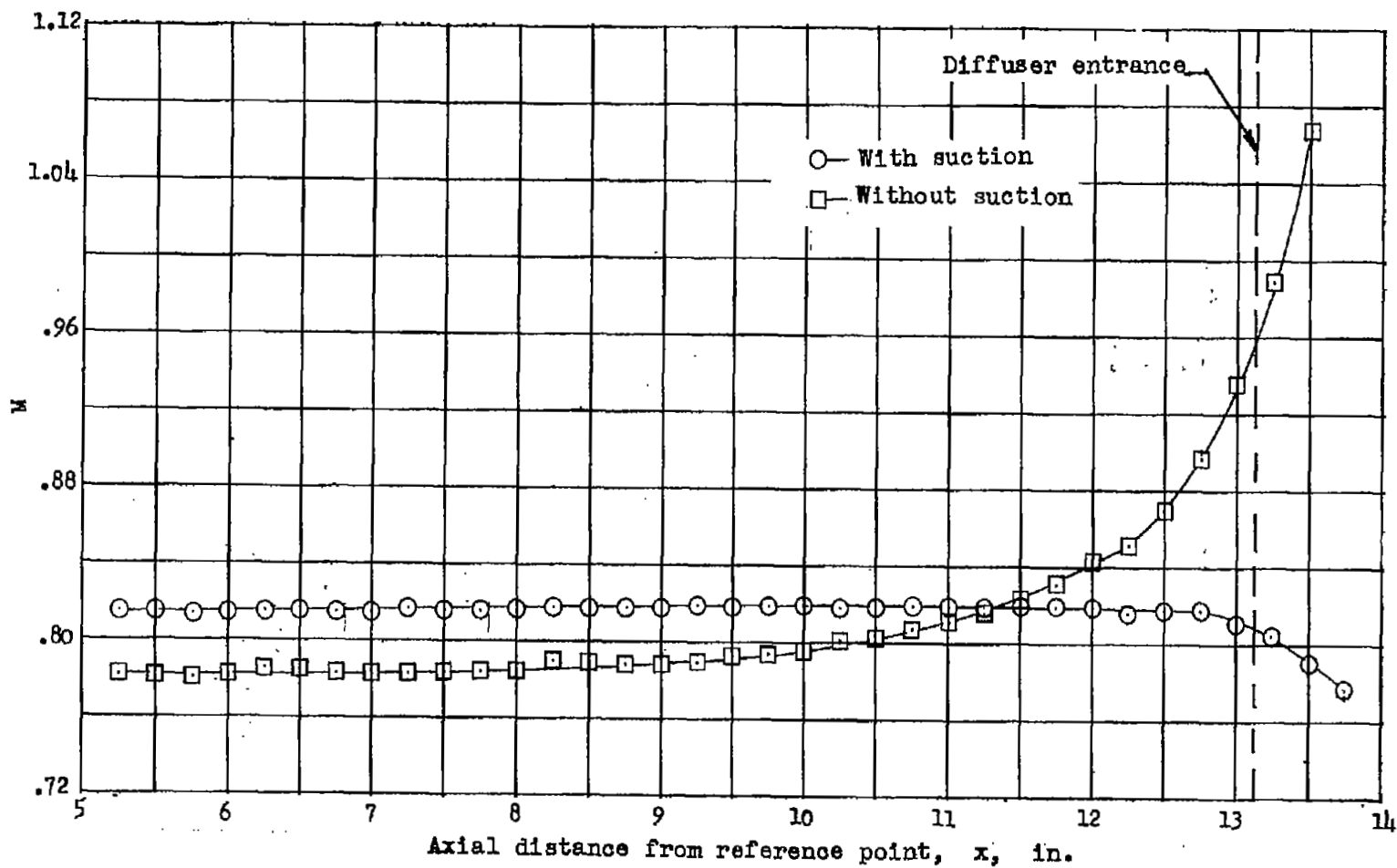


Figure 14.- A comparison of the center-line Mach number distribution with and without suction. Wall divergence angle, 0'; flow guide 2.

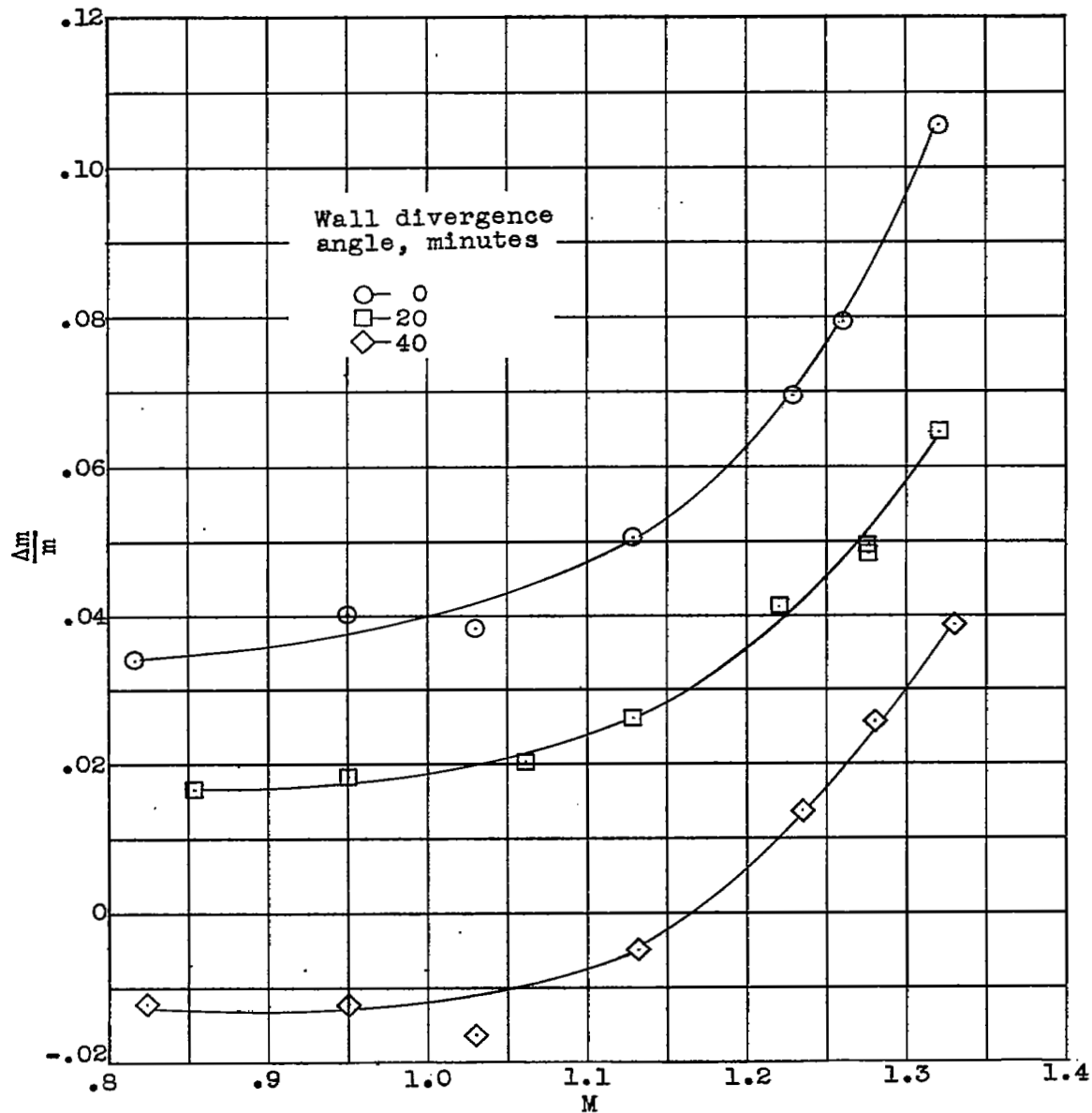


Figure 15.- The suction outflow required to generate various Mach numbers for three wall divergence angles. Flow guide 2.

SECURITY INFORMATION

~~CONFIDENTIAL~~

LANGLEY RESEARCH CENTER  
  
3 1176 01357 2301

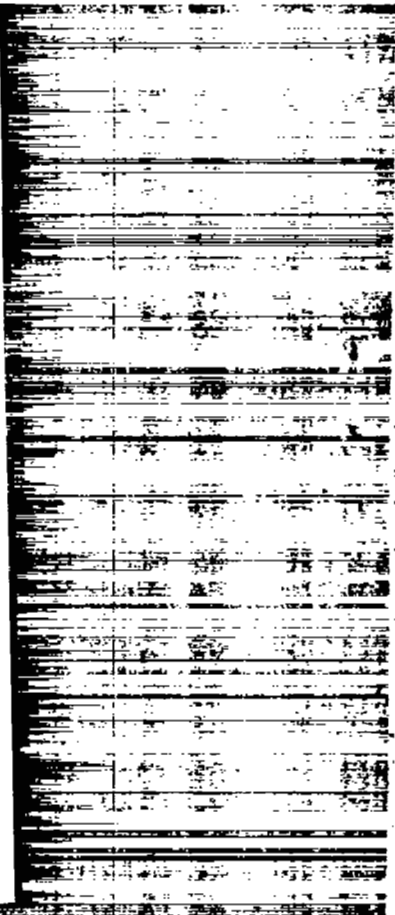
**DO NOT REMOVE SLIP FROM MATERIAL**

Delete your name from this slip when returning material to the library.

NAME	MS

NASA Langley (Rev. May 1988)

RIAD N-75



~~CONFIDENTIAL~~